
FACULTAD DE FÍSICA

DEPARTAMENTO DE FÍSICA ATÓMICA, MOLECULAR Y NUCLEAR

# Design and optimisation of irreversible heat engines

UNIVERSIDAD DE SEVILLA

Irene Prieto Rodríguez

2022-2023

Doble Grado en Física y Matemáticas

---

Supervised by

Carlos Alberto Plata Ramos and Antonio Prados Montaño

# Agradecimientos

Quiero dar las gracias a todas las personas que, de una forma u otra, han hecho posible este trabajo. Especialmente a mis tutores, Carlos Plata y Antonio Prados, que me han guiado magistralmente con su sabiduría y cercanía. Ha sido para mí un placer y un honor poder contar con sus excelentes consejos e inestimable ayuda. Siempre con buen humor, me han hecho sentir muy apoyada en todo momento y, desde luego, este trabajo no habría sido posible sin ellos.

También quiero agradecer su labor a todos los profesores que, a lo largo de mi vida, me han ayudado a formarme tanto en el aspecto académico como humano. Tal vez muchos de ellos no sean del todo conscientes de la gran huella que dejan en sus alumnos, haciéndonos descubrir nuevas formas de ver el mundo y despertando la curiosidad por responder a preguntas que ni nos habíamos podido plantear.

Durante estos años, he tenido la suerte de aprender física y matemáticas junto a maravillosos compañeros, ya amigos, que han hecho que esta etapa, a veces dura, haya sido mucho más amena y feliz. Compartir tiempo, inquietudes y alegrías con ellos ha sido un verdadero regalo.

Y, por supuesto, quiero dar también las gracias a mi familia, que con su apoyo y cariño incondicionales me han enseñado las lecciones más importantes de la vida.

# Resumen

Las máquinas térmicas son dispositivos que convierten energía térmica en trabajo útil operando de manera cíclica. Durante siglos, han desempeñado un papel fundamental en el desarrollo industrial y tecnológico. Históricamente, se han empleado únicamente gases y líquidos como sustancia de trabajo, pero los avances técnicos alcanzados en las últimas décadas permiten ampliar las posibilidades experimentales y diseñar también máquinas que operan con una única partícula. Los sistemas de interés en este caso no pueden tratarse a nivel macroscópico y su estudio se enmarca en el campo de la termodinámica estocástica.

En este trabajo estudiamos máquinas térmicas mesoscópicas constituidas por una partícula browniana confinada en un potencial armónico e inmersa en un fluido que actúa como baño térmico. Diseñamos un ciclo análogo al clásico motor de Stirling, compuesto por dos ramas isotermas y dos isócoras. Nos centramos en el caso irreversible, no cuasi-estático, cuya duración finita permite al dispositivo generar una potencia no nula. Este aspecto es crucial, pues permite plantear la optimización de nuestro ciclo para maximizar la potencia producida, respondiendo así a un interés relevante a nivel práctico. Buscamos los protocolos de control del dispositivo que llevan a la optimalidad, utilizando herramientas del cálculo variacional y de la teoría del control óptimo. Asimismo, exploramos numéricamente la dependencia de la potencia máxima obtenida y la eficiencia correspondiente con los parámetros que caracterizan nuestro sistema.

# Abstract

Heat engines transform thermal energy into useful work, operating in a cyclic manner. For centuries, they have played a key role in industrial and technological development. Historically, only gases and liquids have been used as working substances, but the technical advances achieved over the past decades allow for expanding the experimental possibilities and designing engines operating with a single particle as well. In this case, the systems of interest cannot be addressed at a macroscopic level and their study is framed in the field of stochastic thermodynamics.

In the present work, we study mesoscopic heat engines built with a Brownian particle submitted to harmonic confinement and immersed in a fluid acting as a thermal bath. We design a Stirling-like heat engine, composed of two isothermal and two isochoric branches. We focus on the irreversible, non quasi-static, case—whose finite duration enables the device to deliver a non-zero power output. This is a crucial aspect, inasmuch as it permits to put forward the optimisation of our cycle in order to maximise the delivered power, thereby addressing a relevant interest at a practical level. We search for driving protocols yielding optimality by using tools from variational calculus and optimal control theory. Likewise, we explore numerically the dependence of the maximum power output and the corresponding efficiency on the parameters characterising our system.

# Contents

# Chapter 1

# Introduction

Classical thermodynamics is devoted to the study of heat and related properties in macroscopic systems. The effective conversion of thermal energy into mechanical work was a key factor in the course of the industrial revolution, where the development of steam engines played a major role. Blossoming in the 19th century, the field of classical thermodynamics is governed by a concise set of well-known universal laws, which were stated thanks to the work of scientists such as Sadi Carnot or Rudolf Clausius, culminating in an axiomatic formulation schemed by Constantine Carathéodory [1].

Statistical mechanics, primarily thanks to the contributions of Ludwig Boltzmann, unravelled the probabilistic nature lying underneath the principles of equilibrium thermodynamics. Therein, the macroscopic character of the systems of interest allows for neglecting all the fluctuations involved. At the opposite end, pursuing a deterministic microscopic description of a complex system is, besides unattainable, inessential. Finding an adequate separation between the relevant variables in a physical problem and those whose effect can be encoded by a stochastic noise, causing random fluctuations, is one of the cornerstones of statistical mechanics. With this aim, one typically focuses on an intermediate level of description between the microscopic and macroscopic scales: the mesoscopic one.

Since its inception, statistical mechanics has gone beyond equilibrium, studying a broad and diverse ensemble of physical systems and leading to numerous interdisciplinary applications ranging from plasma physics to modelling biomolecular dynamics. A colloidal particle immersed in a fluid at equilibrium, known as Brownian particle, embodies a paradigmatic system in this wide framework. Its multiple collisions with the tiny particles composing the surrounding fluid give rise to the random Brownian motion.

As the size of a system is reduced, the importance of fluctuations grows, since they may become of the same order of magnitude as the meaningful average values. Present-day miniaturisation of technological devices has brought increasing attention to the extension of thermodynamic results to the mesoscale. Stochastic thermodynamics addresses this

challenging goal, extending concepts such as heat, work and entropy to individual fluctuating trajectories governed by stochastic equations of motion, thereby incorporating time into the study of thermodynamic processes. Furthermore, this fluctuating nature gives rise to novel phenomena with no analogy in the macroscopic world, such as the occurrence of 'transient' violations of the second law of thermodynamics or super Carnot efficiencies in some of the above-mentioned individual trajectories [2,3]. Notwithstanding, the average physical quantities do obey the corresponding universal laws. Moreover, key concepts in thermodynamics, such as that of adiabaticity, require a careful translation to stochastic thermodynamics, with the impossibility of connecting certain states and the emergence of a speed limit for finite-time adiabatic processes [4].

Leveraging the unavoidable fluctuations in a mesoscopic system in order to extract work, as a Maxwell's demon would do [5], constitutes a revolutionary idea that has been deeply studied —both theoretically and experimentally— in the last decades. Recent advances in novel sensing and manipulation techniques in the micro and nanometre length scales, such as optical trapping, have allowed experimental physicists to transfer originally gedanken experiments, analogous to Feynman's ratchet and pawl or Szilard's engine, to actual laboratories [6, 7]. Indeed, we are now equipped to engineer small heat engines performed with a single colloidal particle. Stochastic thermodynamics provides the adequate framework for the design of such mesoscopic heat engines. Finding convenient driving protocols (in terms of delivered power, efficiency, or time duration) for this type of systems has been a major topic in the field [4,8,9]. In addition, interesting connections between information and thermodynamics have arisen as a consequence of the study of feedback protocols [6].

Researchers have explored multiple shortcuts for connecting equilibrium states faster than the corresponding natural relaxation time of the system at hand, often finding inspiration in quantum-control ideas [10,11]. Thus, building mesoscopic finite-time counterparts of classical thermodynamic engines (such as the Carnot, Stirling or Otto cycles) has become a relevant line of research in the field. In reminiscence of its paradigmatic classical counterpart, Carnot-like heat engines have been mainly studied [12–14], encouraging the analysis of other thermal engines as well.

The final objective of the present work is to build an irreversible Stirling cycle. The corresponding classical version, invented and patented by engineer Robert Stirling in 1816, encompasses two isothermal and two isochoric branches. Here, we analyse how this motor can be implemented with a Brownian particle in a harmonic trap. Furthermore, we study how the delivered power can be optimised. This purpose is not only theoretically meaningful, but also worthwhile in practice: experimental realisations of Stirling cycles are achievable [15] and their optimisation may be useful in the search of innovative methods for renewable energy production [16].

# Chapter 2

# The model system

## 2.1 Harmonically confined Brownian particle

We consider an overdamped Brownian particle immersed in a thermal bath at temperature $T$ and trapped in a one-dimensional harmonic potential of stiffness $k$. Both of these parameters are externally controlled. The friction coefficient is denoted as $\lambda$ and it is considered as constant. This assumption is consistent with the experimental realisation of the model: a colloidal particle in an optical trap, where the friction coefficient is determined by both the particle geometry and the solvent viscosity.[1]

Let $x$ denote the particle's position with respect to the centre of the trap. Its evolution follows the Langevin equation

$$\lambda \frac{dx}{dt}(t) = -k(t)x(t) + \zeta(t), \tag{2.1}$$

where $\zeta$ is a Gaussian white noise, characterised by a null average value and a temperature dependent autocorrelation function,

$$\langle \zeta(t) \rangle = 0, \quad \langle \zeta(t)\zeta(t') \rangle = 2\lambda k_B T(t)\delta(t-t'). \tag{2.2}$$

In the above equation, $k_B$ is the Boltzmann constant and $\delta$ is the Dirac delta function.

The stochastic dynamics of the system can be equivalently described in the Fokker-Planck or Langevin formalisms. In order to show this equivalence, we study the evolution of the position's probability distribution in both levels of description.

[1] Actually, recent experimental realisations of colloidal heat engines operate at constant 'physical' temperature and effective kinetic temperatures are implemented by means of external random forces, whose amplitude is controlled. Albeit the friction coefficient $\lambda$ could depend on the physical temperature, the use of an effective kinetic temperature ensures that considering $\lambda$ as a constant is a rather sensible assumption.

### 2.1.1 Fokker-Planck description

This formalism is based on the Fokker-Planck equation [17, 18], which governs the probability density function $P(x,t)$ of finding the Brownian particle at position $x$ in the time instant $t$, and reads

$$\frac{\partial}{\partial t}P(x,t) = \frac{\partial}{\partial x}\left[\frac{k(t)x}{\lambda}P(x,t)\right] + \frac{k_BT(t)}{\lambda}\frac{\partial^2}{\partial x^2}P(x,t). \tag{2.3}$$

In the case of overdamped Brownian motion, the Fokker-Planck equation is also known as the Smoluchowski equation. For the case of harmonic confinement, it can be solved for any given initial distribution $P(x,0)$. Specifically, we derive the solution for a Gaussian initial condition of mean value $\mu_0$ and variance $\sigma_0^2$,

$$P(x,0) = \frac{1}{\sqrt{2\pi\sigma_0^2}}\exp\left[-\frac{(x-\mu_0)^2}{2\sigma_0^2}\right]. \tag{2.4}$$

In Fourier space, the characteristic function corresponding to the probability distribution $P(x,t)$ is defined as

$$G(\xi,t) \equiv \mathcal{F}\left[P(x,t)\right](\xi) = \int_{-\infty}^{+\infty} dx\, e^{i\xi x}P(x,t), \tag{2.5}$$

which is the moment generating function. This name refers to the relation between its derivatives with respect to $\xi$ and the moments of the distribution,

$$G(\xi,t) = \sum_{n=0}^{\infty}\frac{(i\xi)^n}{n!}\langle x^n\rangle(t) \Rightarrow \langle x^n\rangle(t) = \frac{1}{i^n}\frac{\partial G(\xi,t)}{\partial \xi^n}\bigg|_{\xi=0}.$$

Let us recall the expressions of the Fourier transforms of the derivatives involved in Eq. (2.3),

$$\mathcal{F}\left[\frac{\partial}{\partial t}P(x,t)\right](\xi) = \frac{\partial}{\partial t}G(\xi,t), \tag{2.6}$$

$$\mathcal{F}\left[\frac{\partial}{\partial x}P(x,t)\right](\xi) = -i\xi G(\xi,t), \tag{2.7}$$

$$\mathcal{F}\left[\frac{\partial}{\partial x}\left(xP\left(x,t\right)\right)\right](\xi) = -\xi\frac{\partial}{\partial \xi}G(\xi,t). \tag{2.8}$$

Therefore, the problem of solving the Smoluchowski equation (2.3) with an initial Gaussian condition, given in Eq. (2.4), can be equivalently formulated in Fourier space as

follows,

$$\begin{cases} \dfrac{\partial}{\partial t}G(\xi,t) = -\dfrac{k(t)}{\lambda}\xi\dfrac{\partial}{\partial \xi}G(\xi,t) - \dfrac{k_BT(t)}{\lambda}\xi^2 G(\xi,t), \\ \\ \quad G(\xi,0) = \exp\Big[i\mu_0\xi + \frac{1}{2}\sigma_0^2\xi^2\Big]. \end{cases} \tag{2.9}$$

By defining the cumulant generating function

$$\Lambda(\xi,t) = \log G(\xi,t), \tag{2.10}$$

the problem given in Eq. (2.9) can be rewritten as

$$\begin{cases} \dfrac{\partial}{\partial t}\Lambda(\xi,t) = -\dfrac{k(t)}{\lambda}\xi\dfrac{\partial}{\partial \xi}\Lambda(\xi,t) - \dfrac{k_BT(t)}{\lambda}\xi^2, \\ \\ \quad \Lambda(\xi,0) = i\mu_0\xi + \dfrac{1}{2}\sigma_0^2\xi^2. \end{cases} \tag{2.11}$$

We shall consider the power series expansion of the cumulant generating function,

$$\Lambda(\xi,t) = \sum_{n=1}^{\infty} c_n(t)\frac{(i\xi)^n}{n!}, \tag{2.12}$$

from which the cumulants $c_n(t)$ are obtained. Substituting Eq. (2.12) in Eq. (2.11), one easily derives the evolution equations for all the cumulants, which are fully uncoupled. Specifically, for $n = 1$, we have

$$\begin{cases} i\xi\dfrac{dc_1}{dt}(t) = i\xi\dfrac{k(t)}{\lambda}c_1(t) \Rightarrow \dfrac{dc_1}{dt}(t) = -\dfrac{k(t)}{\lambda}c_1(t), \\ \\ \quad c_1(0) = \mu_0. \end{cases} \tag{2.13}$$

Hence, the first cumulant, which is the position's mean value, can be readily obtained,

$$\langle x\rangle(t) \equiv c_1(t) = \mu_0 e^{-\frac{1}{\lambda}K(t)}, \tag{2.14}$$

where $K$ is a primitive function of $k$ defined as

$$K(t) \equiv \int_0^t dt' k(t'). \tag{2.15}$$

For $n = 2$, one gets

$$\begin{cases} -\dfrac{1}{2}\xi^2\dfrac{dc_2}{dt}(t) = \dfrac{k(t)}{\lambda}\xi^2 c_2(t) - \dfrac{k_BT(t)}{\lambda}\xi^2 \Rightarrow \dfrac{dc_2}{dt}(t) = -\dfrac{2k(t)}{\lambda}c_2(t) + \dfrac{2k_BT(t)}{\lambda}, \\ \\ \quad c_2(0) = \sigma_0^2. \end{cases} \tag{2.16}$$

Therefore, the second cumulant, which is the variance of the distribution, is

$$\langle x^2\rangle(t) - \langle x\rangle^2(t) = c_2(t) = e^{-\frac{2}{\lambda}K(t)}\left[\sigma_0^2 + \frac{2k_B}{\lambda}\int_0^t dt'\, e^{\frac{2}{\lambda}K(t')}T(t')\right]. \tag{2.17}$$

Since the selected initial probability distribution is Gaussian, all cumulants $c_n(0)$ for $n \geq 3$ vanish. Given that, in addition, Eq. (2.11) does not have any independent terms going as $\xi^n$ for $n \neq 2$, the power expansion of the aforementioned problem for $n \geq 3$ gives an homogeneous equation with null initial value, yielding the trivial solution $c_n(t) = 0$. Thus, we can write the evolution of the cumulants in a compact manner,

$$c_n(t) = \begin{cases} \mu_0 e^{-\frac{1}{\lambda}K(t)}, & n = 1, \\ e^{-\frac{2}{\lambda}K(t)}\left[\sigma_0^2 + \frac{2k_B}{\lambda}\int_0^t dt'\, e^{\frac{2}{\lambda}K(t')}T(t')\right], & n = 2, \\ 0, & n \geq 3. \end{cases} \tag{2.18}$$

Therefore, an initial Gaussian condition guarantees that the probability density function remains Gaussian at any time instant. Thence, it suffices to characterise the evolution of both the mean value and the variance of the particle's position to fully depict the time evolution of the probability density function $P(x,t)$. Equation (2.14) proves that the mean value $\langle x\rangle$ vanishes at any time instant if the position origin is selected according to the initial mean value, coinciding with the centre of the trap, $\mu_0 = 0 = \langle x\rangle$. Thus, the position distribution evolution is entirely encoded by that of its variance—which, given that $\langle x\rangle(t) = 0\ \forall t$, coincides with the second moment of the distribution. Thence, it is governed by Eq. (2.16), equivalent to

$$\begin{cases} \lambda\dfrac{d}{dt}\langle x^2\rangle(t) = -2k(t)\langle x^2\rangle(t) + 2k_B T(t), \\ \langle x^2\rangle(0) = \sigma_0^2. \end{cases} \tag{2.19}$$

### 2.1.2 Langevin description

All of the results presented above can be analogously derived using the Langevin approach. Given a Gaussian initial distribution for $x(0)$, we can deduce that $x(t)$ is also Gaussian. Indeed, since the initial condition $x(0)$ and the noise $\zeta(t)$ are both Gaussian, Eq. (2.1) entails that the particle position remains Gaussian.

The Langevin equation (2.1) can be straightforwardly solved,

$$x(t) = \left[x_0 + \frac{1}{\lambda}\int_0^t dt'\zeta(t')e^{K(t')/\lambda}\right]e^{-K(t)/\lambda}, \tag{2.20}$$

where $x_0$ is the position of the particle in the initial time instant (i.e. $x_0 \equiv x(t=0)$), and $K$ is defined as in Eq. (2.15). Therefore, the position's mean value is

$$\langle x \rangle (t) = \langle x_0 \rangle e^{-K(t)/\lambda}, \tag{2.21}$$

as we obtained in Eq. (2.14), where we denoted $\langle x_0 \rangle = \mu_0$.

From Eq. (2.20), the squared value of the position of the Brownian particle can be readily computed,

$$x^2(t) = \left[ x_0^2 + \frac{2x_0}{\lambda} \int_0^t dt' \zeta(t') e^{K(t')/\lambda} + \frac{1}{\lambda^2} \int_0^t dt' \zeta(t') e^{K(t')/\lambda} \int_0^t dt'' \zeta(t'') e^{K(t'')/\lambda} \right] e^{-2K(t)/\lambda}. \tag{2.22}$$

Now, the second moment of the distribution is easily obtained bearing in mind the properties of the Gaussian white noise (2.2),

$$\begin{aligned} \langle x^2 \rangle (t) = \Bigg[ & \left\langle x_0^2 \right\rangle + \frac{2\langle x_0 \rangle}{\lambda} \int_0^t dt' \underbrace{\langle \zeta(t') \rangle}_{0} e^{K(t')/\lambda} \\ & + \frac{1}{\lambda^2} \int_0^t dt' \int_0^t dt'' \underbrace{\langle \zeta(t') \zeta(t'') \rangle}_{2\lambda k_B T(t) \delta(t-t')} e^{\frac{K(t')+K(t'')}{\lambda}} \Bigg] e^{-2K(t)/\lambda} \\ = & \left[ \left\langle x_0^2 \right\rangle + \frac{2k_B}{\lambda} \int_0^t dt' T(t') e^{2K(t')/\lambda} \right] e^{-2K(t)/\lambda}. \end{aligned} \tag{2.23}$$

Hence, the time evolution of this physical quantity is determined by the following equation,

$$\lambda \frac{d}{dt} \langle x^2 \rangle (t) = -2k(t) \langle x^2 \rangle (t) + 2k_B T(t). \tag{2.24}$$

Thereupon, we retrieve the time evolution of the second moment captured in Eq. (2.19). As aforementioned, a proper choice of the origin in our coordinate system gives $\langle x_0 \rangle = 0$, thereby the variance and the second moment coincide and the above equation suffices to fully determine the evolution of the position distribution of our Brownian particle.

### 2.1.3 Energy, work and heat

In the described system, the three-dimensional phase space $(k, \langle x^2 \rangle, T)$ is considered. The implicit equation defining the equilibrium surface in this space, which is called *equation of state*, can be directly obtained by looking for the stationary solution of Eq. (2.24), when both the stiffness and the temperature are time-independent,

$$0 = -2k \langle x^2 \rangle_{eq} + 2k_B T \Rightarrow \langle x^2 \rangle_{eq} = \frac{k_B T}{k}. \tag{2.25}$$

The energy of the system has a kinetic term and a configurational contribution derived from the harmonic potential,

$$E(t) = \frac{1}{2}mv^2(t) + \frac{1}{2}k(t)x^2, \tag{2.26}$$

where $m$ is the mass of the Brownian particle and $v$ is its velocity. In the overdamped limit, which corresponds to our description, the latter variable is always at its equilibrium value: $v^2(t) = k_B T(t)/m$. Therefore, the average energy is

$$\langle E\rangle(t) = \frac{1}{2}k_B T(t) + \frac{1}{2}k(t)\langle x^2\rangle(t). \tag{2.27}$$

Thus, the equilibrium energy is characterised by the temperature of the system,

$$\langle E\rangle_{eq} = k_B T. \tag{2.28}$$

Taking differentials on both sides of Eq. (2.27), one gets

$$d\langle E\rangle = \underbrace{\frac{1}{2}k_B\, dT + \frac{1}{2}k\, d\langle x^2\rangle}_{đQ} + \underbrace{\frac{1}{2}dk\,\langle x^2\rangle}_{đW}. \tag{2.29}$$

We can identify work's inexact differential $đW$ as the contribution to the energy variation stemming from the change of the external mechanical parameters (namely, the stiffness of the trap $k$). The energy variation caused by a configurational change in the probability distributions is depicted as the heat's inexact differential $đQ$. It includes two terms, each of which corresponds to the change in the variance of the particle's velocity or position. Since the former variable, as aforementioned, is always at equilibrium, the associated variation term is directly connected to the temperature change. Although we focus here on heat and work as average energy contributions, the corresponding stochastic quantities can also be defined on individual fluctuating trajectories.

Let us consider a process connecting two equilibrium state points: $(k_i, \langle x^2\rangle_i, T_i)$ and $(k_f, \langle x^2\rangle_f, T_f)$, where the subscripts denote the initial and final situations, respectively. Work and heat associated to this transition are defined as follows,

$$W_{i\to f} = \frac{1}{2}\int_i^f dk\,\langle x^2\rangle, \tag{2.30}$$

$$Q_{i\to f} = \frac{1}{2}\int_i^f \left(k_B\, dT + k\, d\langle x^2\rangle\right) = \frac{k_B}{2}(T_f - T_i) + \frac{1}{2}\int_i^f k\, d\langle x^2\rangle. \tag{2.31}$$

Note that our sign convention considers any 'kind' of energy change (both work and heat) as positive if it is transferred from the environment to the system, and negative in the opposite case. Since our objective is to extract energy from our heat engine, we thus

study cycles with a negative total work. The first law of thermodynamics is expressed as

$$\Delta\langle E\rangle_{i\to f} = W_{i\to f} + Q_{i\to f}, \tag{2.32}$$

where $\Delta\langle E\rangle_{i\to f} = \langle E\rangle_f - \langle E\rangle_i$.

## 2.2 Dimensionless variables

In order to simplify our notation, let us introduce dimensionless variables for the physical properties that characterise our three-dimensional phase space. Specifically, we choose the units of $(k, \langle x^2\rangle, T)$ to be normalised with respect to a reference equilibrium point $(k_{\rm ref}, \langle x^2\rangle_{\rm ref}, T_{\rm ref})$, i.e.

$$\kappa \equiv \frac{k}{k_{\rm ref}}, \quad y \equiv \frac{\langle x^2\rangle}{\langle x^2\rangle_{\rm ref}} = \frac{k_{\rm ref}}{k_B T_{\rm ref}}\langle x^2\rangle, \quad \theta \equiv \frac{T}{T_{\rm ref}}. \tag{2.33}$$

Note that the second equality for the normalised variance is a direct consequence of the equilibrium condition (2.25), which now reads

$$\kappa y_{eq} = \theta. \tag{2.34}$$

Consistently, dimensionless average energy is defined,

$$\mathcal{E} = \frac{\langle E\rangle}{k_B T_{\rm ref}}. \tag{2.35}$$

Thereupon, we can rewrite Eq. (2.27) in dimensionless form as

$$\mathcal{E} = \frac{1}{2}\theta + \frac{1}{2}\kappa y, \tag{2.36}$$

where we have omitted the time dependence for the sake of clarity. Non-dimensional work and heat are defined consistently,

$$\mathcal{W}_{i\to f} = \frac{1}{2}\int_i^f d\kappa\, y, \tag{2.37}$$

$$\mathcal{Q}_{i\to f} = \frac{1}{2}(\theta_f - \theta_i) + \frac{1}{2}\int_i^f dy\, \kappa. \tag{2.38}$$

The first law of thermodynamics now reads

$$\Delta\mathcal{E}_{i\to f} = \mathcal{W}_{i\to f} + \mathcal{Q}_{i\to f}. \tag{2.39}$$

In addition, it is useful to adimensionalise time as follows,

$$\tau \equiv \frac{t\, k_{\mathrm{ref}}}{\lambda}. \tag{2.40}$$

The state of the system at any time $\tau$ is thus characterised by the triplet $(\kappa, y, \theta)$. From now on, differentiation with respect to $\tau$ is denoted as $\dot{q} \equiv dq/d\tau$, for any physical quantity $q$. Hence, the evolution of the non-dimensional variance follows the equation

$$\dot{y} = -2\kappa y + 2\theta. \tag{2.41}$$

With the previous definitions, we can write Eq. (2.17) as

$$y(\tau) = e^{-2\int_0^\tau d\tau\, \kappa(\tau')} \left[ y_i + 2 \int_0^\tau d\tau'\, \theta(\tau') e^{2\int_0^{\tau'} d\tau''\, \kappa(\tau'')} \right], \tag{2.42}$$

which gives us the evolution of the variance. Note that, for the special case of constant stiffness $\kappa$ and temperature $\theta$, we have that the variance exponentially decays to its equilibrium value,

$$y(\tau) = \frac{\theta}{\kappa} + e^{-2\kappa\tau} \left( y_i - \frac{\theta}{\kappa} \right). \tag{2.43}$$

Thus, if we consider an infinitely slow process (compared to the characteristic relaxation time of our system), the stiffness of the trap and the temperature behave as constants in our time-scale and the second term on the rhs vanishes. Thence, the normalised variance attains its equilibrium value. This situation corresponds to the quasi-static limit, which will be studied in the upcoming chapters.

# Chapter 3

# Building blocks for a Stirling cycle

The aim of this work is to build and investigate a non-equilibrium version of the Stirling cycle, in analogy to the studies of irreversible Carnot-like heat engines [12–14]. Hence, our stochastic cycle should encompass isothermal and isochoric branches. In the following, we define and analyse in detail these branches.

## 3.1 Isothermal processes

In phase space, isothermal processes are represented by curves with a constant value for $\theta$. In this work, we consider two kinds of isothermal processes: quasi-static and optimal. The former is not our main interest; not only are quasi-static processes non-feasible experimentally, but also they lack practical interest, due to their null output power. However, the study of quasi-static transitions is theoretically meaningful, and it is essential to compare both scenarios. Nevertheless, our focus is the power optimisation of an irreversible heat engine, and hence isothermal processes in which the extracted work is maximised play a key role.

### 3.1.1 Quasi-static isothermal processes

A quasi-static process is defined as a succession of equilibrium states [1]. Therefore, an isothermal quasi-static process is represented by an equilibrium curve of the form given in Eq. (2.34), in which the temperature $\theta$ is fixed. To sweep this equilibrium curve $y(\tau) = \theta/\kappa(\tau)$, the control parameter $\kappa(\tau)$ must be varied sufficiently slowly. For a quasi-static process, the work required to drive the system from one state to another always equals the Helmholtz free energy difference between the initial and final points $\Delta F_{i\to f}$, which is a function of state.

The computation of work, heat and energy variation in such a process is straightforward,

$$\mathcal{W}_{i\to f}^{QS} = \frac{1}{2}\int_i^f d\kappa\,\frac{\theta}{\kappa} = \frac{\theta}{2}\log\left(\frac{\kappa_f}{\kappa_i}\right) = \Delta F_{i\to f}, \tag{3.1}$$

$$\mathcal{Q}_{i\to f}^{QS} = \frac{1}{2}\int_i^f dy\frac{\theta}{y} = \frac{\theta}{2}\log\left(\frac{y_f}{y_i}\right) = -\frac{\theta}{2}\log\left(\frac{\kappa_f}{\kappa_i}\right) = -\mathcal{W}_{i\to f}^{QS}, \tag{3.2}$$

$$\Delta\mathcal{E}_{i\to f}^{QS} = 0. \tag{3.3}$$

The last equality can be derived as a consequence of the first law, or directly remembering that $\mathcal{E}_i = \mathcal{E}_f = \theta$ for an isothermal process.

### 3.1.2 Optimal isothermal processes

Let us consider an isothermal process lasting a finite time $\tau_f$. In such a protocol, the system sweeps non-equilibrium states and thus work depends on the selected protocol for the control $\kappa(\tau)$. Therefore, it is possible to minimise the work performed on the system (i.e. maximise the work done by the system) by finding an optimal protocol $\kappa(\tau)$. This optimisation problem has already been solved in Ref. [12]. Hereafter, we revisit the obtaining of such optimal isothermal protocol.

Work is a functional of the engineered protocol,

$$\mathcal{W}_{i\to f}[\kappa] = \frac{1}{2}\int_i^f d\kappa\, y = \frac{1}{2}\cancelto{0}{\Big[y\kappa\Big]_i^f} - \frac{1}{2}\int_i^f dy\,\kappa, \tag{3.4}$$

where integration by parts leads to the second equality. Note that the first term on the rhs vanishes, due to the equilibrium condition at the initial and final states: $\kappa_i y_i = \kappa_f y_f = \theta$. Similarly to the quasi-static case, we have that $\mathcal{E}_i = \mathcal{E}_f = \theta$ and thus

$$\mathcal{Q}_{i\to f}[\kappa] = -\mathcal{W}_{i\to f}[\kappa], \quad \Delta\mathcal{E}_{i\to f} = 0. \tag{3.5}$$

The evolution equation of the variance, captured in Eq. (2.41), yields

$$\kappa = \frac{\theta}{y} - \frac{1}{2}\frac{\dot{y}}{y}. \tag{3.6}$$

Introducing this relation in Eq. (3.4), one obtains

$$\mathcal{W}_{i\to f}[\kappa] = -\frac{\theta}{2}\int_i^f d(\log y) + \frac{1}{4}\int_i^f d\tau\frac{\dot{y}^2}{y} = \Delta F_{i\to f} + \frac{1}{4}\int_i^f d\tau\frac{\dot{y}^2}{y}. \tag{3.7}$$

The first term in the last expression does not depend on the selected protocol, given that it is the free energy difference, i.e. the quasi-static contribution. Hence, since it is a function of state, its value is determined by the boundary point states, which are fixed. Thereupon, the optimisation problem is solely determined by the second term, which is the 'irreversible' or 'excess' work, i.e. the difference between the actual work and its value in the quasi-static, reversible, limit. Note that, as expected, the irreversible contribution is positive regardless of the selected protocol.

Let us introduce the 'Lagrangian'

$$\mathcal{L}(y,\dot{y}) = \frac{\dot{y}^2}{y}. \tag{3.8}$$

The Euler-Lagrange equation corresponding to our variational problem, i.e. the minimisation of the irreversible work, is

$$\frac{d}{d\tau}\frac{\partial \mathcal{L}}{\partial \dot{y}} - \frac{\partial \mathcal{L}}{\partial y} = 0 \iff 2\ddot{y}\,y - \dot{y}^2 = 0. \tag{3.9}$$

The solution of this second-order differential equation is obtained by standard methods, with the result

$$y(\tau) = (a\tau + b)^2, \tag{3.10}$$

where $(a,b)$ are integration constants. They can be determined by imposing the boundary conditions $y(0) = y_i$, $y(\tau_f) = y_f$,

$$y_i = b^2 \Rightarrow b = \sqrt{y_i}, \tag{3.11}$$

$$y_f = (a\tau_f + b)^2 \Rightarrow a = \frac{1}{\tau_f}\left(\sqrt{y_f} - \sqrt{y_i}\right). \tag{3.12}$$

Hence, the evolution of the variance in the optimal process is

$$\tilde{y}(\tau) = \left[\sqrt{y_i} + \left(\sqrt{y_f} - \sqrt{y_i}\right)\frac{\tau}{\tau_f}\right]^2, \quad \forall \tau \in [0,\tau_f]. \tag{3.13}$$

We observe that $\tilde{y}(\tau)$ is continuous in the closed interval $[0,\tau_f]$ and it is a positive-defined quantity, as the variance of any distribution must be.

The control $\tilde{\kappa}$ evolution in the optimal process is obtained from Eq. (3.6), in the open time interval $\tau \in (0,\tau_f)$,

$$\tilde{\kappa}(\tau) = \frac{\theta}{\tilde{y}(\tau)} - \frac{1}{2}\frac{d}{d\tau}\log\tilde{y}(\tau) = \frac{\theta}{\left[\sqrt{y_i} + \left(\sqrt{y_f} - \sqrt{y_i}\right)\frac{\tau}{\tau_f}\right]^2} - \left[\tau + \frac{\tau_f}{\left(\sqrt{y_f/y_i} - 1\right)}\right]^{-1}. \tag{3.14}$$

Note that the stiffness of the trap is discontinuous at both the initial and final time

instants,

$$\lim_{\tau\to 0^+}\tilde{\kappa}(\tau) = \kappa_i - \frac{1}{\tau_f}\left(\sqrt{\frac{y_f}{y_i}} - 1\right) \neq \kappa_i, \tag{3.15}$$

$$\lim_{\tau\to \tau_f^-}\tilde{\kappa}(\tau) = \kappa_f - \frac{1}{\tau_f}\left(1 - \sqrt{\frac{y_i}{y_f}}\right) \neq \kappa_f. \tag{3.16}$$

Similar discontinuities in the control parameter have been repeatedly found in stochastic thermodynamics [9,11,12,14,19]. Note that the continuity at the boundaries is recovered in the quasi-static limit, in which $\tau_f \to \infty$.

Work associated with the optimal process is obtained from Eq. (3.4),

$$\widetilde{\mathcal{W}}_{i\to f} = \mathcal{W}^{QS}_{i\to f} + \frac{1}{\tau_f}\left(\sqrt{y_f} - \sqrt{y_i}\right)^2 = \mathcal{W}^{QS}_{i\to f} + \frac{\theta}{\tau_f}\left(\frac{1}{\sqrt{\kappa_f}} - \frac{1}{\sqrt{\kappa_i}}\right)^2. \tag{3.17}$$

The work does not only depend on the initial and final equilibrium states connected by the isothermal process, but also on the duration of such transition. The minimum irreversible work scales as $\tau_f^{-1}$, which vanishes in the quasi-static limit $\tau_f \to \infty$.

We recall that, according to our sign convention, work delivered by the heat engine is negative. Hence, when we refer to 'optimal work', we are talking about a minimum value. In Eq. (3.17), we obtain that the optimal work is always greater (i.e. 'worse' in energetic exploitation terms) than the corresponding quasi-static value. Albeit the extracted work is maximum in the quasi-static limit, it leads to a vanishing power output. The opposite limit, an instantaneous isothermal transition ($\tau_f \to 0^+$), leads to the least energetically advantageous case: infinite work is required to perform the process.

## 3.2 Isochoric processes

In this section, our focus of interest are processes in which the harmonic potential is kept constant.[1] They are represented by curves with a fixed value for the trap stiffness $\kappa$ in the phase space. Similarly to our treatment of isothermal branches, we will study quasi-static and optimal isochoric transitions. In this case, optimality refers to shortest time protocols, given that work vanishes for any isochoric process. Hence, minimal time will imply maximal power output.

Therefore, isochoric processes are particularly simple: since the required work is always zero, heat is fully determined by the temperature difference between the final and initial

[1] In reminiscence of macroscopic heat engines operating with gases, our nomenclature exploits the analogy between $(\kappa, y)$ and volume and pressure $(V, p)$. Consequently, an isochoric process—associated with constant $V$ in gases—corresponds here to keeping $\kappa$ constant.

states, and so is the energy variation,

$$\mathcal{W}_{i\to f} = \frac{1}{2}\int_i^f d\kappa\, y = 0, \tag{3.18}$$

$$\mathcal{Q}_{i\to f} = \frac{1}{2}\int_i^f dy\,\kappa + \frac{1}{2}(\theta_f - \theta_i) = \underbrace{\frac{\kappa}{2}(y_f - y_i)}_{\kappa(y_f-y_i)=\theta_f-\theta_i} + \frac{1}{2}(\theta_f - \theta_i) = \theta_f - \theta_i, \tag{3.19}$$

$$\Delta\mathcal{E}_{i\to f} = \mathcal{W}_{i\to f} + \mathcal{Q}_{i\to f} = \theta_f - \theta_i. \tag{3.20}$$

As one may intuitively expect, the system delivers heat to the bath in cooling processes ($\theta_f < \theta_i$) and absorbs heat from the bath in heating ones ($\theta_f > \theta_i$).

### 3.2.1 Quasi-static isochoric processes

In order to sweep a quasi-static curve, the control parameter, which in this case is the bath temperature $\theta(\tau)$, shall be tuned in an infinitely slow manner in order to maintain the equilibrium condition $y(\tau) = \theta(\tau)/\kappa$. As outlined above, the energetic characterisation of the isochoric process is identical for any given protocol, independently of the duration of the process or whether the intermediate states are at equilibrium or not.

### 3.2.2 Optimal isochoric processes

We now aim at studying the thermal optimal protocol that minimises the connection time between the equilibrium initial and final states, keeping the potential fixed. This optimal shortcut has been investigated in depth in Ref. [9]. Therein, the problem is solved for arbitrary dimension, which yields a rich phenomenology. Hereupon, we restrict ourselves to the one-dimensional case that we are considering throughout.

The external control $\theta(\tau)$ is submitted to physical constraints, $\theta(\tau) \geq 0$, $\forall\tau$. But, moreover, tighter bounds might be brought up by technical limitations in practice. Thus, we consider the general constraints $\theta_{\min} \leq \theta(\tau) \leq \theta_{\max}$ for the bath temperature to solve the optimisation problem, particularising later for the ideally relaxed conditions $\theta_{\min} \to 0^+$, $\theta_{\max} \to \infty$. The addressed optimisation problem cannot be solved with the tools of standard variational calculus and less restrictive methods of optimal control theory are needed. The solution of our problem is a bang-bang protocol without 'switchings' (i.e. with a single continuity interval), in which $\theta(\tau)$ is equal to one of its bounds. A detailed derivation of this result can be found in Appendix A. Therein, we obtain that the optimal temperature control in a heating process corresponds to reaching the upper

bound, $\tilde{\theta}(\tau) = \theta_{\max}$, $\forall \tau \in (0, \tau_f)$; whereas, in a cooling procedure, optimality is achieved by setting the temperature control to its lower bound, $\tilde{\theta}(\tau) = \theta_{\min}$, $\forall \tau \in (0, \tau_f)$. Thus, the optimal control $\tilde{\theta}(\tau)$ can be expressed as

$$\tilde{\theta}(\tau) = \tilde{\theta} \equiv \begin{cases} \theta_{\max}, & \text{if} \quad \theta_i < \theta_f, \\ \theta_{\min}, & \text{if} \quad \theta_i > \theta_f, \end{cases} \qquad \forall \tau \in (0, \tau_f)\,. \tag{3.21}$$

Note that, again, our optimal control presents jumps: $\tilde{\theta}(\tau)$ is discontinuous at the initial and final time instants, given that it is submitted to the boundary conditions

$$\tilde{\theta}(0) = \theta_i, \quad \tilde{\theta}(\tau_f) = \theta_f. \tag{3.22}$$

The optimal protocol is physically reasonable: it coincides with the intuitive idea of using the largest or smallest possible bath temperatures—depending on whether one intends to heat or cool the system, respectively. Then, one just needs to select the adequate temperature bound and wait until the target state is reached. Since the optimal control is constant in the open interval $(0, \tau_f)$, it is particularly easy to solve the evolution equation for the variance of the confined Brownian particle, obtaining

$$\tilde{y}(\tau) = \frac{\tilde{\theta}}{\kappa} + \left( y_i - \frac{\tilde{\theta}}{\kappa} \right) e^{-2\kappa\tau}, \quad \forall \tau \in (0, \tau_f)\,, \tag{3.23}$$

where $\tilde{\theta}$ is given by Eq. (3.21). The optimal time connection is obtained by solving the equation

$$y_f = \lim_{\tau \to \tau_f^-} \tilde{y}(\tau) = \frac{\tilde{\theta}}{\kappa} + \left( y_i - \frac{\tilde{\theta}}{\kappa} \right) e^{-2\kappa\tau_f}, \tag{3.24}$$

or, equivalently after dividing by $y_f$,

$$1 = \frac{\tilde{\theta}}{\theta_f} + \left( \frac{\theta_i}{\theta_f} - \frac{\tilde{\theta}}{\theta_f} \right) e^{-2\kappa\tau_f}, \tag{3.25}$$

where we have taken into account that $y_f = \kappa\theta_f$, since the final state verifies the equilibrium condition. This equation can be readily solved, yielding an optimal time

$$\widetilde{\tau}_f = -\frac{1}{2\kappa} \log \left( \frac{\theta_f - \tilde{\theta}}{\theta_i - \tilde{\theta}} \right). \tag{3.26}$$

Therefore, considering the expression of $\tilde{\theta}$ given in Eq. (3.21), one has

$$\widetilde{\tau}_f = \begin{cases} \dfrac{1}{2\kappa}\log\left(\dfrac{\theta_{\max}-\theta_i}{\theta_{\max}-\theta_f}\right), & \text{if} \quad \theta_i < \theta_f, \\ \dfrac{1}{2\kappa}\log\left(\dfrac{\theta_i-\theta_{\min}}{\theta_f-\theta_{\min}}\right), & \text{if} \quad \theta_i > \theta_f. \end{cases} \tag{3.27}$$

The argument of the logarithmic function is greater than 1 in both cases, thus, the obtained optimal value $\tau_f$ is always positive, as it must be. Note that an opposite selection in Eq. (3.21) (i.e. choosing the largest temperature of the bath for cooling processes and the minimal temperature for heating), besides of being a physically unreasonable choice, would turn into a negative connection time. Thereof, our choosing in Eq. (3.21) has been proven to be correct. It is worth highlighting that, although the control parameter $\tilde{\theta}(\tau)$ is not continuous at both ends of the isochoric process, the associated optimal variance $\tilde{y}$ is continuous in the whole time interval, since its expression, given in Eq. (3.23), verifies

$$\lim_{\tau\to 0^+}\tilde{y}(\tau) = y_i, \quad \lim_{\tau\to\tau_f^-}\tilde{y}(\tau) = y_f. \tag{3.28}$$

The energetic analysis of this optimal isochoric process is identical to the quasi-static one, given that work is null and heat and energy variation only depend on the boundary temperatures. As previously mentioned, the key difference between the quasi-static and optimal isochoric processes is that the latter lasts a finite time, whereas the former involves an infinite duration.

In our discussion, we are particularly interested in the ideal situation $\theta_{\min}\to 0^+$, $\theta_{\max}\to\infty$, for which the minimum connecting time in an isochoric process is

$$\widetilde{\tau}_f = \begin{cases} \lim\limits_{\theta_{\max}\to\infty}\dfrac{1}{2\kappa}\log\left(\dfrac{\theta_{\max}-\theta_i}{\theta_{\max}-\theta_f}\right) = 0, & \text{if} \quad \theta_i < \theta_f, \\ \lim\limits_{\theta_{\min}\to 0^+}\dfrac{1}{2\kappa}\log\left(\dfrac{\theta_i-\theta_{\min}}{\theta_f-\theta_{\min}}\right) = \dfrac{1}{2\kappa}\log\left(\dfrac{\theta_i}{\theta_f}\right), & \text{if} \quad \theta_i > \theta_f. \end{cases} \tag{3.29}$$

Thus, in the ideal limit of infinite heating power, it is possible to instantaneously heat the system up to any desired temperature; while the physical bound for minimal temperatures leads to a non-zero finite limit of the optimal time for cooling processes.

# Chapter 4

# Stirling stochastic heat engine

In this chapter, we study the stochastic version of a Stirling cycle performed by our model system. Experimental versions of such engines have been experimentally built in the last decades [3, 15].

Analogously to the classical Stirling heat engine, our cyclic process encompasses four stages, which are illustrated in Fig. 4.1:

1. **Isothermal expansion** at the hot bath temperature $\theta_h \equiv \theta_A = \theta_B$, connecting the phase points $A$ and $B$, i.e. $(\kappa_A, y_A, \theta_A)$ and $(\kappa_B, y_B, \theta_B)$. The confining harmonic potential is modified via time control of the trap strength $\kappa(\tau)$. Here and onwards, the term *expansion* (*compression*) refers to the sign of the variance increment: $\Delta y > 0$ ($\Delta y < 0$), in analogy to the classical thermodynamic cycle.

2. **Isochoric compression** at 'loose' stiffness $\kappa_l \equiv \kappa_B = \kappa_C$, starting from the state-point $B \equiv (\kappa_B, y_B, \theta_B)$ up to $C \equiv (\kappa_C, y_C, \theta_C)$. The time-dependence of the temperature of the heat bath $\theta(\tau)$ is now controlled.

3. **Isothermal compression** at the cold bath temperature $\theta_c \equiv \theta_C = \theta_D < \theta_h$, linking states $C \equiv (\kappa_C, y_C, \theta_C)$ and $D \equiv (\kappa_D, y_D, \theta_D)$. Similarly to process 1, the stiffness of the harmonic trap is externally controlled.

4. **Isochoric expansion** at 'tight' stiffness $\kappa_t \equiv \kappa_D = \kappa_A > \kappa_l$, departing from state $D \equiv (\kappa_D, y_D, \theta_D)$ and closing the cycle by returning to the initial point $A \equiv (\kappa_A, y_A, \theta_A)$. As in process 2, the control variable is the time-dependent temperature of the bath.

Since the energy increment in an isothermal process vanishes, from the application of the first law of thermodynamics, we infer that in branches 1 and 3 the absorbed (released) heat equals the delivered (consumed) work,

$$\mathcal{W}_{AB} = -\mathcal{Q}_{AB} < 0, \qquad \mathcal{W}_{CD} = -\mathcal{Q}_{CD} > 0. \tag{4.1}$$

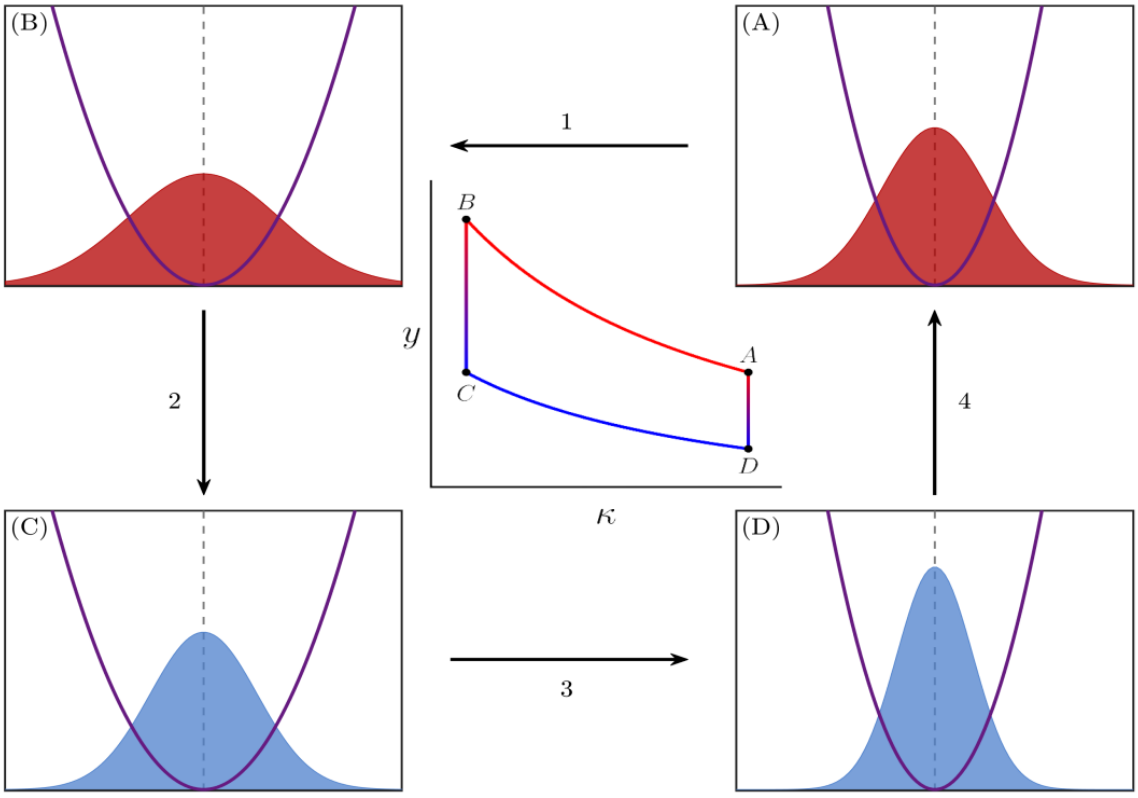


**Figure 4.1: Scheme of the stochastic Stirling cycle.** The harmonic confining potential at the operating points of the cycle is represented by the purple curves. The filled red and blue areas correspond to the probability density functions at those state-points, where red (blue) refers to the hot (cold) equilibrium temperatures. The representation of the heat engine in the $(\kappa, y)$ plane correspond to the quasi-static version of the described cycle.

As we mentioned in the previous chapter, isochoric processes do not generate nor require work, and therein the associated dissipated heat equals the temperature increment. We recall that these energetic considerations apply to any isochoric process, independently of the protocol for the temperature. Therefore, we have the following identities for branches 2 and 4 of our cycle:

$$\mathcal{W}_{BC} = 0, \qquad \mathcal{Q}_{BC} = \theta_C - \theta_B = \theta_c - \theta_h < 0; \tag{4.2}$$

$$\mathcal{W}_{DA} = 0, \qquad \mathcal{Q}_{DA} = \theta_A - \theta_D = \theta_h - \theta_c > 0. \tag{4.3}$$

We are interested in building a heat engine, and thus we want our device to extract heat from the baths and perform work. On one hand, the absorbed heat corresponds to the first isothermal branch $A \to B$: $\mathcal{Q}_{AB}$. On the other hand, the total work transferred from the environment to our Stirling cycle is

$$\mathcal{W} \equiv \mathcal{W}_{AB} + \cancelto{0}{\mathcal{W}_{BC}} + \mathcal{W}_{CD} + \cancelto{0}{\mathcal{W}_{DA}} = \mathcal{W}_{AB} + \mathcal{W}_{CD}. \tag{4.4}$$

The efficiency of our stochastic heat machine is defined, in analogy with macroscopic thermodynamics, as the ratio of the performed work over the extracted heat,

$$\eta \equiv \frac{-\mathcal{W}}{\mathcal{Q}_{AB}} = \frac{-\left(\mathcal{W}_{AB} + \mathcal{W}_{CD}\right)}{\mathcal{Q}_{AB}} = 1 - \frac{\mathcal{W}_{CD}}{\mathcal{Q}_{AB}} < 1. \tag{4.5}$$

Let us denote the time duration of each branch as $\tau_{AB}$, $\tau_{BC}$, $\tau_{CD}$, $\tau_{DA}$. Thence, the delivered power of the cycle, defined as the ratio of the performed work over the employed time, is

$$\mathcal{P} \equiv \frac{-\mathcal{W}}{\tau_{AB} + \tau_{BC} + \tau_{CD} + \tau_{DA}} = \frac{-\left(\mathcal{W}_{AB} + \mathcal{W}_{CD}\right)}{\tau_{AB} + \tau_{BC} + \tau_{CD} + \tau_{DA}}. \tag{4.6}$$

If we temporarily forgot about the constraints to which our engine is submitted, we would expect that $4 \times 3 = 12$ parameters were necessary to fully depict the cycle characterised by 4 points in a 3-dimensional phase space. Nonetheless, we now consider normalisation on the phase space coordinates with respect to the initial state, and thence point $A$ is fixed: $(\kappa_A, y_A, \theta_A) = (1, 1, 1)$. Furthermore, the operating points describe equilibrium states and thus the corresponding condition, given in Eq. (2.34), imposes three additional constraints,

$$\kappa_B y_B = \theta_B, \quad \kappa_C y_C = \theta_C, \quad \kappa_D y_D = \theta_D. \tag{4.7}$$

Moreover, as a consequence of the processes being isothermal and isochoric, two more pairs of restrictions are added,

$$\theta_A = \theta_B, \qquad \theta_C = \theta_D, \tag{4.8}$$

$$\kappa_B = \kappa_C, \qquad \kappa_A = \kappa_D. \tag{4.9}$$

**Table 4.1:** Operating points of the stochastic Stirling heat engine. See also Fig. 4.2.

| | $\kappa$ | $y$ | $\theta$ |
|---|---|---|---|
| $A$ | 1 | 1 | 1 |
| $B$ | $\chi$ | $\chi^{-1}$ | 1 |
| $C$ | $\chi$ | $\nu\chi^{-1}$ | $\nu$ |
| $D$ | 1 | $\nu$ | $\nu$ |

Accordingly, the operating points of the described Stirling cycle are uniquely defined by two parameters. Similarly to the choice of parameters in Ref. [14], we characterise the device using the temperature ratio between the cold and heat baths,

$$\nu \equiv \frac{\theta_c}{\theta_h} = \theta_c < 1, \tag{4.10}$$

and the compression ratio among the two isochoric branches,

$$\chi \equiv \frac{\kappa_l}{\kappa_s} = \kappa_l < 1. \tag{4.11}$$

The phase coordinates of the operating points of the cycle as a function of the selected variables $(\nu, \chi)$ are collected in Table 4.1.

## 4.1 Quasi-static Stirling cycle

We first study the quasi-static limit of the designed cycle. Therein, the system is always at equilibrium and the time required to sweep the cycle is infinite. The analysis of isothermal and isochoric quasi-static processes discussed in the previous chapter allows for straightforward calculating work, heat and energy increases over each branch. The obtained values are collected in Table 4.2. The total work corresponding to this infinitely slow process is

$$\mathcal{W}^{QS} \equiv \frac{1-\nu}{2} \log \chi < 0. \tag{4.12}$$

Since the required time for this engine to operate is infinite, it does not deliver any power. As mentioned in the previous chapter, this quasi-static limit is not experimentally realisable. Nonetheless, the efficiency of such device attains the Carnot efficiency,

$$\eta^{QS} = \eta_C \equiv 1 - \frac{\theta_c}{\theta_h} = 1 - \nu, \tag{4.13}$$

**Table 4.2:** Quasi-static energetics of the Stirling cycle.

| | | $\mathcal{W}^{QS}_{i\to f}$ | $\mathcal{Q}^{QS}_{i\to f}$ | $\Delta\mathcal{E}^{QS}_{i\to f}$ |
|---|---|---|---|---|
| (1) | $A \to B$ | $\frac{1}{2}\log\chi$ | $-\frac{1}{2}\log\chi$ | 0 |
| (2) | $B \to C$ | 0 | $\nu - 1$ | $\nu - 1$ |
| (3) | $C \to D$ | $-\frac{\nu}{2}\log\chi$ | $\frac{\nu}{2}\log\chi$ | 0 |
| (4) | $D \to A$ | 0 | $1 - \nu$ | $1 - \nu$ |
| Total | | $\frac{1-\nu}{2}\log\chi$ | $\frac{\nu-1}{2}\log\chi$ | 0 |

which is the maximum achievable thermal efficiency, as stated by Carnot's theorem, which can be derived as a consequence of the second law of thermodynamics. A corollary of the aforementioned theorem proves that all reversible engines operating between the same hot and cold reservoirs are equally efficient. Thus, the equality provided in Eq. (4.13) between the efficiency of our quasi-static, reversible, heat engine and the Carnot efficiency is consistent with the results of macroscopic thermodynamics.

The projection of the described quasi-static cycle onto the $(\kappa, y)$ plane in the phase space is illustrated on the left panel in Fig. 4.2, for the particular choice of parameters $\nu = \chi = 0.5$.

## 4.2 Optimal irreversible Stirling cycle

Let us consider now the irreversible version of the above described stochastic Stirling cycle. Now, the four branches are swept in a finite time and the heat engine delivers thus a non-zero power output. As anticipated in previous sections, our aim is to build the 'optimal' irreversible cycle for any given operating points $(A, B, C, D)$; i.e. the cycle that delivers maximum power for any choice of temperature and compression ratios $(\nu, \chi)$. Therefore, these parameters are considered as constants in the following.

Henceforth, our objective is to maximise the power output of the cycle, which is given by Eq. (4.6). Inasmuch as the isochoric branches only contribute to the delivered power through their time spans, we must minimise their duration in order to achieve our goal. We have already addressed this problem in detail in Sec. 3.2.2 of the previous chapter. Therein, we obtained that the optimal temperature protocol is of bang-bang type, and it consists of applying the minimal bath temperature in the cooling branch (i.e. $B \to C$) and using the maximum bath temperature in the heating branch (i.e. $D \to A$).

This procedure leads to the following optimal times for the isochoric brachistochrones

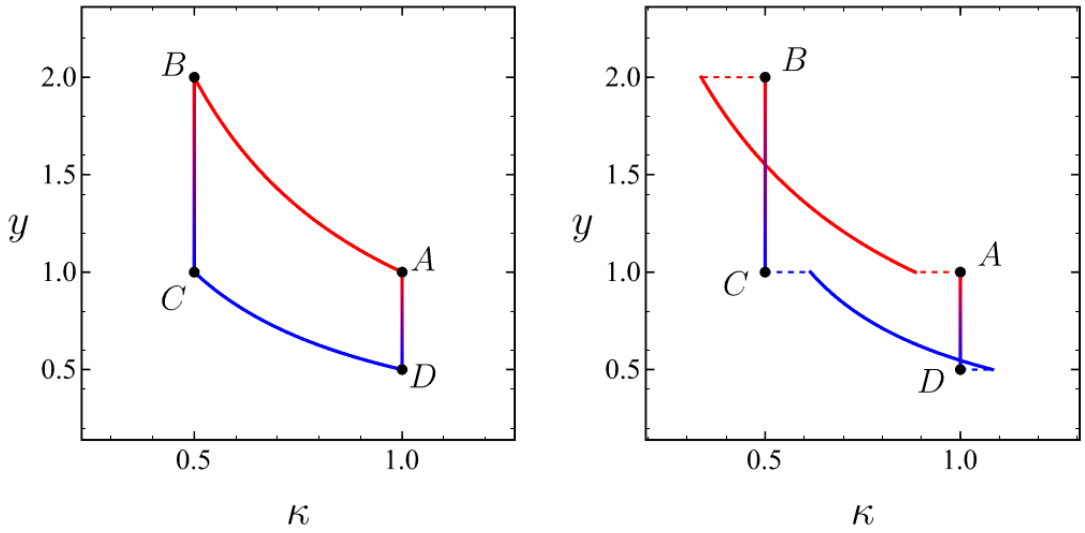


**Figure 4.2:** Projection onto the $(\kappa, y)$ plane of the phase trajectory described by the system in the Stirling cycle. The left (right) panel corresponds to the reversible (irreversible) versions of the cycle. In both panels, the cycles correspond to $\nu = \chi = 0.5$; for the irreversible cycle, we have considered that the bounds for the temperature are ideal: $\theta_{\min} \to 0^+$, $\theta_{\max} \to \infty$.

connecting, respectively, $B \to C$ and $D \to A$,

$$\widetilde{\tau}_{BC}(\theta_{\min}) = \frac{1}{2\chi} \log\left(\frac{1-\theta_{\min}}{\nu-\theta_{\min}}\right), \qquad \widetilde{\tau}_{DA}(\theta_{\max}) = \frac{1}{2} \log\left(\frac{\theta_{\max}-\nu}{\theta_{\max}-1}\right), \tag{4.14}$$

which are directly obtained from Eq. (3.29). Here, we have explicitly showed the dependence of these optimal times on the extremal admissible bath temperatures. Let us denote the total optimal time for the isochoric branches as

$$\widetilde{\tau}_{\text{isoc}} \equiv \widetilde{\tau}_{BC} + \widetilde{\tau}_{DA}, \tag{4.15}$$

where we have omitted the dependence on $(\theta_{\min}, \theta_{\max})$ in our notation for the sake of simplicity.

Regarding the isothermal branches, in order to optimise the cycle power given in Eq. (4.6), we need to minimise the irreversible work in these processes (or, equivalently, maximise the work performed by the system). In the previous chapter, specifically in Sec. 3.1.2, we derived the optimal protocol for this type of processes for any given time duration. We obtained that the stiffness $\kappa$ experimented finite jump discontinuities at the endpoints of these isothermal processes. This behaviour is shown on the right panel in Fig. 4.2, where the dashed lines represent the aforementioned jumps. The optimal work

for these processes as a function of their time span is

$$\widetilde{\mathcal{W}}_{AB}(\tau_{AB}) = \frac{1}{2}\log\chi + \frac{1}{\tau_{AB}}\left(\frac{1}{\sqrt{\chi}} - 1\right)^2, \tag{4.16}$$

$$\widetilde{\mathcal{W}}_{CD}(\tau_{CD}) = -\frac{\nu}{2}\log\chi + \frac{\nu}{\tau_{CD}}\left(1 - \frac{1}{\sqrt{\chi}}\right)^2, \tag{4.17}$$

which are a direct consequence of Eq. (3.17).

Therefore, the optimal protocols for the isochoric branches are fixed by the bath parameters and the optimal protocols for the isothermal connections are only dependent on their respective times. Naturally, we may now ask ourselves what are the times $\widetilde{\tau}_{AB}, \widetilde{\tau}_{CD}$ that make our device deliver maximum power,

$$\widetilde{\mathcal{P}} = \max_{\tau_{AB},\tau_{CD}} \mathcal{P}\left(\tau_{AB}, \tau_{CD}\right), \tag{4.18}$$

where

$$\mathcal{P}\left(\tau_{AB}, \tau_{CD}\right) \equiv -\frac{\widetilde{\mathcal{W}}_{AB}(\tau_{AB}) + \widetilde{\mathcal{W}}_{CD}(\tau_{CD})}{\tau_{AB} + \widetilde{\tau}_{BC} + \tau_{CD} + \widetilde{\tau}_{DA}} = -\frac{\widetilde{\mathcal{W}}_{AB}(\tau_{AB}) + \widetilde{\mathcal{W}}_{CD}(\tau_{CD})}{\tau_{AB} + \widetilde{\tau}_{\text{isoc}} + \tau_{CD}}. \tag{4.19}$$

To answer this question, let us rewrite Eq. (4.19) as follows,

$$\begin{aligned}\mathcal{P}\left(\tau_{AB}, \tau_{CD}\right) &= -\frac{1}{\tau_{\text{cyc}}}\left[\frac{1-\nu}{2}\log\chi + \left(\frac{1}{\sqrt{\chi}} - 1\right)^2\left(\frac{1}{\tau_{AB}} + \frac{\nu}{\tau_{CD}}\right)\right] \\ &= -\frac{1}{\tau_{\text{cyc}}}\left[\mathcal{W}^{QS} + \alpha\left(\frac{1}{\tau_{AB}} + \frac{\nu}{\tau_{CD}}\right)\right],\end{aligned} \tag{4.20}$$

where $\mathcal{W}^{QS}$ is the total work corresponding to the quasi-static cycle, given in Eq. (4.12),

$$\tau_{\text{cyc}} \equiv \tau_{AB} + \widetilde{\tau}_{\text{isoc}} + \tau_{CD} \tag{4.21}$$

is the total duration of the cycle, and the coefficient $\alpha$ is defined as

$$\alpha \equiv \left(\frac{1}{\sqrt{\chi}} - 1\right)^2, \tag{4.22}$$

for the sake of compactness.

We maximise the power by imposing the necessary conditions for optimality, i.e. making the partial derivatives of $\mathcal{P}$ with respect to $\tau_{AB}$ and $\tau_{CD}$ equal to zero,

$$\left.\frac{\partial\mathcal{P}}{\partial\tau_{AB}}\right|_{\widetilde{\tau}_{AB},\widetilde{\tau}_{CD}} = 0 \iff \frac{1}{(\widetilde{\tau}_{\text{cyc}})}\frac{\alpha}{\widetilde{\tau}_{AB}^2} + \frac{1}{(\widetilde{\tau}_{\text{cyc}})^2}\left[\mathcal{W}^{QS} + \alpha\left(\frac{1}{\widetilde{\tau}_{AB}} + \frac{\nu}{\widetilde{\tau}_{CD}}\right)\right] = 0, \tag{4.23}$$

$$\left.\frac{\partial \mathcal{P}}{\partial \tau_{CD}}\right|_{\widetilde{\tau}_{AB},\widetilde{\tau}_{CD}} = 0 \iff \frac{1}{(\widetilde{\tau}_{\rm cyc})}\frac{\alpha\nu}{\widetilde{\tau}_{CD}^2} + \frac{1}{(\widetilde{\tau}_{\rm cyc})^2}\left[\mathcal{W}^{QS} + \alpha\left(\frac{1}{\widetilde{\tau}_{AB}} + \frac{\nu}{\widetilde{\tau}_{CD}}\right)\right] = 0. \tag{4.24}$$

Both Eq. (4.23) and Eq. (4.24) must be verified by the optimal times. Therefore, subtracting both equations, we infer that the optimal times for the isothermal branches are proportional,

$$\frac{\alpha}{(\widetilde{\tau}_{\rm cyc})}\left[\frac{1}{\widetilde{\tau}_{AB}^2} - \frac{\nu}{\widetilde{\tau}_{CD}^2}\right] = 0 \Rightarrow \widetilde{\tau}_{CD} = \sqrt{\nu}\,\widetilde{\tau}_{AB}, \tag{4.25}$$

where we have taken into account that $\alpha > 0$, since $\chi < 1$, and $\widetilde{\tau}_{AB}, \widetilde{\tau}_{CD} > 0$.

Thus, multiplying Eq. (4.23) by $(\widetilde{\tau}_{\rm cyc})^2\widetilde{\tau}_{AB}^2 > 0$ and using the relation in Eq. (4.25) to express $\widetilde{\tau}_{CD}$ as a function of $\widetilde{\tau}_{AB}$, one has

$$\mathcal{W}^{QS}\widetilde{\tau}_{AB}^2 + 2\alpha\left(1+\sqrt{\nu}\right)\widetilde{\tau}_{AB} + \alpha\widetilde{\tau}_{\rm isoc} = 0. \tag{4.26}$$

This is a simple quadratic equation, the solution of which is

$$\widetilde{\tau}_{AB} = \frac{\alpha}{\mathcal{W}^{QS}}\left[-\left(1+\sqrt{\nu}\right) - \sqrt{\left(1+\sqrt{\nu}\right)^2 - \frac{\mathcal{W}^{QS}}{\alpha}\widetilde{\tau}_{\rm isoc}}\right], \tag{4.27}$$

where we have selected the solution with negative sign before the square root to ensure positivity of the optimal time: $\widetilde{\tau}_{AB} > 0$ (remember that $\mathcal{W}^{QS} > 0$). Let us introduce the new parameters

$$w \equiv -\frac{\mathcal{W}^{QS}}{\alpha\left(1+\sqrt{\nu}\right)^2} > 0, \qquad \sigma \equiv \sqrt{1 + w\widetilde{\tau}_{\rm isoc}} > 1, \tag{4.28}$$

in order to simplify the resulting expressions. With these definitions, we have

$$\widetilde{\tau}_{AB} = \frac{1+\sigma}{w\left(1+\sqrt{\nu}\right)}, \quad \widetilde{\tau}_{CD} = \sqrt{\nu}\,\frac{1+\sigma}{w\left(1+\sqrt{\nu}\right)}, \tag{4.29}$$

which are equivalent to Eqs. (4.27) and (4.25).

Therefore, we have solved the optimisation problem presented in Eq. (4.18) and the optimal irreversible Stirling cycle is fully characterised for any given operation points and extremal bath temperatures $(\theta_{\rm min}, \theta_{\rm max})$. Note that we have not explicitly written the dependence of the optimal solution on the latter, which is encoded in the parameter $\sigma$ by means of $\widetilde{\tau}_{\rm isoc} = \widetilde{\tau}_{\rm isoc}(\theta_{\rm min}, \theta_{\rm max})$. The corresponding protocols for the trap stiffness $\kappa(\tau)$ in the isothermal branches and the bath temperature $\theta(\tau)$ in the isochoric connections have been described in detail in Chapter 3.

The energetics of the designed optimal irreversible Stirling cycle can be readily calculated. In analogy with Table 4.2, which collected the energetic description of the quasistatic limit, we present the corresponding description for the optimal irreversible cycle in

**Table 4.3:** Energetics of the optimal irreversible Stirling cycle.

| | $\widetilde{\mathcal{W}}_{i\to f}$ | $\widetilde{\mathcal{Q}}_{i\to f}$ | $\Delta\widetilde{\mathcal{E}}_{i\to f}$ |
|---|---|---|---|
| (1) $A\to B$ | $\frac{1}{2}\log\chi - \frac{\mathcal{W}^{QS}}{\left(1+\sqrt{\nu}\right)(1+\sigma)}$ | $-\frac{1}{2}\log\chi + \frac{\mathcal{W}^{QS}}{\left(1+\sqrt{\nu}\right)(1+\sigma)}$ | 0 |
| (2) $B\to C$ | 0 | $\nu-1$ | $\nu-1$ |
| (3) $C\to D$ | $-\frac{\nu}{2}\log\chi - \left(\frac{\sqrt{\nu}}{1+\sqrt{\nu}}\right)\frac{\mathcal{W}^{QS}}{1+\sigma}$ | $\frac{\nu}{2}\log\chi + \left(\frac{\sqrt{\nu}}{1+\sqrt{\nu}}\right)\frac{\mathcal{W}^{QS}}{1+\sigma}$ | 0 |
| (4) $D\to A$ | 0 | $1-\nu$ | $1-\nu$ |
| Total | $\frac{\sigma}{1+\sigma}\mathcal{W}^{QS}$ | $-\frac{\sigma}{1+\sigma}\mathcal{W}^{QS}$ | 0 |

Table 4.3. Note that the total work absorbed by the system is

$$\widetilde{\mathcal{W}} = \frac{\sigma}{1+\sigma}\mathcal{W}^{QS}. \tag{4.30}$$

This result exhibits a strong parallelism to the one presented in Ref. [14] for an optimal irreversible Carnot engine. As pointed out therein, the form of Eq. (4.30) yields a physical interpretation for the parameter $\sigma$: it is a measurement of the deviation of the total irreversible work from the value corresponding to the quasi-static case. In the limit $\sigma\to\infty$, one has $\widetilde{\mathcal{W}}\to\mathcal{W}^{QS}$. Note that, from the definition of $\sigma$ in Eq. (4.28), it is clear that the limit $\sigma\to\infty$ corresponds, indeed, to infinitely slow isochoric processes: $\widetilde{\tau}_{\rm isoc}\to\infty$. Consistently, Eq. (4.29) evinces that the limit $\sigma\to\infty$ implies an infinite duration for the optimal isothermal branches as well.

Therefore, the optimal power for any given operating points, defined by the temperature ratio between the hot and cold isotherms $\nu$ and the compression ratio between the isochoric branches $\chi$, is

$$\widetilde{\mathcal{P}} = \left(\frac{\sigma}{1+\sigma}\right)\frac{w\mathcal{W}^{QS}}{1+\sigma+w\widetilde{\tau}_{\rm isoc}}. \tag{4.31}$$

We recall that the optimal time for the isochoric branches $\widetilde{\tau}_{\rm isoc}$ also depends on the bounds of the temperature control. Hence, the optimal time is a function of all the aforementioned parameters, which have been considered as fixed constants in our derivation,

$$\widetilde{\mathcal{P}}\left(\nu,\chi;\,\theta_{\rm min},\theta_{\rm max}\right) = \left[\frac{\sigma\left(\nu,\chi;\,\theta_{\rm min},\theta_{\rm max}\right)}{1+\sigma\left(\nu,\chi;\,\theta_{\rm min},\theta_{\rm max}\right)}\right]\frac{w\left(\nu,\chi\right)\mathcal{W}^{QS}\left(\nu,\chi\right)}{1+\sigma+w\left(\nu,\chi\right)\widetilde{\tau}_{\rm isoc}\left(\nu,\chi;\,\theta_{\rm min},\theta_{\rm max}\right)}. \tag{4.32}$$

In the above expression, we explicitly show where the dependence on these four parameters comes from.

Let us look into the efficiency of the optimised irreversible Stirling cycle,

$$\tilde{\eta} = \frac{-\left(\widetilde{\mathcal{W}}_{AB} + \widetilde{\mathcal{W}}_{CD}\right)}{\widetilde{\mathcal{Q}}_{AB}} = 1 + \frac{\widetilde{\mathcal{W}}_{CD}}{\widetilde{\mathcal{W}}_{AB}}, \tag{4.33}$$

which, similarly to the optimal power $\widetilde{\mathcal{P}}$, depends on $(\nu, \chi; \theta_{\min}, \theta_{\max})$, although we omit this dependency in our notation for the sake of conciseness. We can easily check that the Carnot efficiency $\eta_C = 1 - \nu$ is an upper bound for $\tilde{\eta}$,

$$\begin{aligned}\tilde{\eta} = \eta_C + \frac{\widetilde{\mathcal{W}}_{CD} + \nu\widetilde{\mathcal{W}}_{AB}}{\widetilde{\mathcal{W}}_{AB}} &= \eta_C + \frac{\cancel{-\frac{\nu}{2}\log\chi} - \frac{\sqrt{\nu}\,\mathcal{W}^{QS}}{(1+\sqrt{\nu})(1+\sigma)} + \cancel{\frac{\nu}{2}\log\chi} - \frac{\nu\mathcal{W}^{QS}}{(1+\sqrt{\nu})(1+\sigma)}}{\widetilde{\mathcal{W}}_{AB}} \\ &= \eta_C - \frac{\left(\sqrt{\nu}+\nu\right)\mathcal{W}^{QS}}{\left(1+\sqrt{\nu}\right)(1+\sigma)\,\widetilde{\mathcal{W}}_{AB}} = \eta_C - \underbrace{\left(\frac{\sqrt{\nu}}{1+\sigma}\right)\frac{\mathcal{W}^{QS}}{\widetilde{\mathcal{W}}_{AB}}}_{>0},\end{aligned} \tag{4.34}$$

where the factor within parentheses is clearly positive, and the terms $\mathcal{W}^{QS}$, $\widetilde{\mathcal{W}}_{AB}$ are both negative. We can rewrite the expression of the latter, given in Table 4.3, to make clear that it has a well-defined sign,

$$\begin{aligned}\widetilde{\mathcal{W}}_{AB} &= \frac{1}{2}\log\chi - \frac{\mathcal{W}^{QS}}{\left(1+\sqrt{\nu}\right)(1+\sigma)} = \frac{1}{2}\log\chi\left[1 - \frac{1-\nu}{\left(1+\sqrt{\nu}\right)(1+\sigma)}\right] \\ &= \frac{1}{2}\log\chi\left(1 - \frac{1-\sqrt{\nu}}{1+\sigma}\right) = \underbrace{\frac{1}{2}\log\chi}_{<0}\underbrace{\left(\frac{\sigma+\sqrt{\nu}}{1+\sigma}\right)}_{>0} < 0.\end{aligned} \tag{4.35}$$

Nonetheless, a similiar manipulation of Eq. (4.33) shows that the Curzon-Ahlborn efficiency [20]

$$\eta_{CA} \equiv 1 - \sqrt{\nu} \tag{4.36}$$

is not an *upper* but a *lower* bound for our optimal irreversible Stirling cycle. Indeed,

$$\begin{aligned}\tilde{\eta} = \eta_{CA} + \frac{\widetilde{\mathcal{W}}_{CD} + \sqrt{\nu}\,\widetilde{\mathcal{W}}_{AB}}{\widetilde{\mathcal{W}}_{AB}} &= \eta_{CA} + \frac{-\frac{\nu}{2}\log\chi - \frac{\sqrt{\nu}\,\mathcal{W}^{QS}}{(1+\sqrt{\nu})(1+\sigma)} + \frac{\sqrt{\nu}}{2}\log\chi - \frac{\sqrt{\nu}\,\mathcal{W}^{QS}}{(1+\sqrt{\nu})(1+\sigma)}}{\widetilde{\mathcal{W}}_{AB}} \\ &= \eta_{CA} + \frac{1}{\widetilde{\mathcal{W}}_{AB}}\left[\frac{\sqrt{\nu}(1-\sqrt{\nu})}{2}\log\chi - \frac{2\sqrt{\nu}\,\mathcal{W}^{QS}}{\left(1+\sqrt{\nu}\right)(1+\sigma)}\right] \\ &= \eta_{CA} + \frac{\sqrt{\nu}\log\chi}{\widetilde{\mathcal{W}}_{AB}}\left[\frac{1-\sqrt{\nu}}{2} - \frac{1-\nu}{\left(1+\sqrt{\nu}\right)(1+\sigma)}\right] = \eta_{CA} + \underbrace{\frac{\sqrt{\nu}(1-\sqrt{\nu})}{2\widetilde{\mathcal{W}}_{AB}}\log\chi}_{>0}\underbrace{\left(\frac{\sigma-1}{\sigma+1}\right)}_{>0},\end{aligned} \tag{4.37}$$

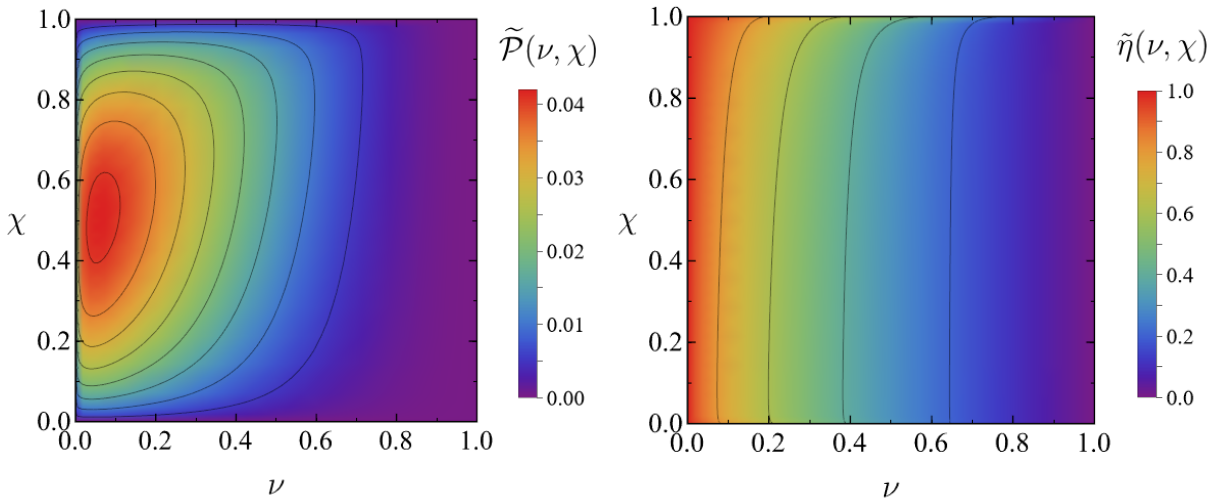


**Figure 4.3:** Density plots of the optimal power (left) and the corresponding efficiency (right) in the $(\nu,\chi)$ plane. We have considered that the bounds for the temperature are $\theta_{\min}\to 0^{+}$, $\theta_{\max}\to\infty$.

where we have taken into account that $\nu<1$ , $\widetilde{\mathcal{W}}_{AB}$ and $\log\chi$ are both negative and $\sigma>1$.

Curzon and Ahlborn found $\eta_{CA}$ to be the efficiency of a Carnot engine operating at maximum power output when limitations in the rates of heat transfer were considered [20]. They derived this result for a specific model, generating a long-standing debate about its universality and validity as an upper bound. Its generality has been discarded, since efficiencies at maximum power below and above $\eta_{CA}$ have been reported in the literature [12,14,21,22]. However, it turns out to be an actual upper bound for the linear response at maximum power, being reached in this regime by systems with strong coupling between work and heat fluxes [23]. We recall that, in linear order, the Curzon-Ahlborn efficiency is exactly half of the Carnot efficiency, $\eta_{CA}=\eta_C/2+O(\eta_C^2)$. Moreover, in the special case of systems with strong coupling between the fluxes, possessing in addition left-right symmetry, the Curzon-Ahlborn result is verified up to quadratic order [21]. Our designed engine is found to operate always above the Curzon-Ahlborn efficiency, as shown by Eq. (4.37).

In order to illustrate the results obtained in this section, density plots of the optimal power and the corresponding efficiency as a function of $(\nu,\chi)$, in the ideal case of $\theta_{\min}\to 0^{+}$, $\theta_{\max}\to\infty$, are presented in Fig. 4.3.

### 4.2.1 Further optimisation of the irreversible Stirling cycle over the operating points

Hitherto, we have studied the optimisation of an irreversible Stirling cycle for which the operating points, defined by the temperature and compression ratios $(\nu,\chi)$, were

fixed. Naturally, the question of what choice of ratios renders maximal power arises, and this section is devoted to answering this question. We first analyse the ideal case of non-technical, but only physical, constraints in the temperature control: $\theta_{\min} \to 0^+$, $\theta_{\max} \to \infty$. Secondly, we focus on more realistic limitations for the thermal control.

#### 4.2.1.1 Optimisation of the irreversible Stirling cycle in the ideal limit

Let us consider an irreversible Stirling cycle with variable operating points in the limit case of an ideal thermal control, i.e. one in which the temperature has no upper bound, $\theta_{\max} \to \infty$, and the lower bound corresponds to the absolute zero, $\theta_{\min} \to 0^+$. The optimal power for any given operating points only depends here on the temperature and compression ratios, $\widetilde{\mathcal{P}} = \widetilde{\mathcal{P}}(\nu, \chi)$.

Herein, we first look into the delivered power optimisation over the compression ratio $\chi$, which will depend on the choice of the temperature ratio $\nu$ between the cold and hot branches of the cycle,

$$\widetilde{\mathcal{P}}^*(\nu) \equiv \max_{\chi\in(0,1)} \widetilde{\mathcal{P}}(\nu,\chi) = \widetilde{\mathcal{P}}\left(\nu, \chi^*(\nu)\right), \tag{4.38}$$

where $\chi^*(\nu)$ denotes the compression ratio yielding optimal power for any fixed temperature ratio $\nu$. Furthermore, we can find the overall optimal Stirling cycle by maximising now $\widetilde{\mathcal{P}}^*$ over the temperature ratio $\nu$,

$$\widetilde{\mathcal{P}}^{**} \equiv \max_{\substack{\chi\in(0,1)\\ \nu\in(0,1)}} \widetilde{\mathcal{P}}(\nu,\chi) = \max_{\nu\in(0,1)} \widetilde{\mathcal{P}}^*(\nu) = \widetilde{\mathcal{P}}\left(\nu^*, \chi^{**}\right) = 0.041, \tag{4.39}$$

where $\nu^* = 0.060$ is the temperature ratio that gives the overall maximum delivered power and $\chi^{**} \equiv \chi^*(\nu^*) = 0.507$ is the corresponding optimal compression ratio.

To illustrate these definitions, we present in Fig. 4.4 the density plot of the optimal power in the $(\nu, \chi)$ plane with the curve $\chi = \chi^*(\nu)$, as well as two plots showing the behaviour of the optimal power as a function of the compression ratio $\chi$ for fixed values of the temperature ratio $\nu \in \{1/2, \nu^*\}$. Interestingly, we find the compression ratio $\chi^*(\nu)$ yielding optimal power for fixed $\nu$ to be monotonically increasing with respect the temperature ratio $\nu$.

Similarly to the optimal power, the efficiency at maximum power for fixed operating points is a function of the temperature and compression ratios, $\tilde{\eta} = \tilde{\eta}(\nu, \chi)$. We denote the efficiency corresponding to the power optimisation over the compression ratio and to the overall maximum power in an analogous manner,

$$\tilde{\eta}^*(\nu) \equiv \tilde{\eta}\left(\nu, \chi^*(\nu)\right), \quad \tilde{\eta}^{**} \equiv \tilde{\eta}\left(\nu^*, \chi^{**}\right) = 0.842, \tag{4.40}$$

respectively.

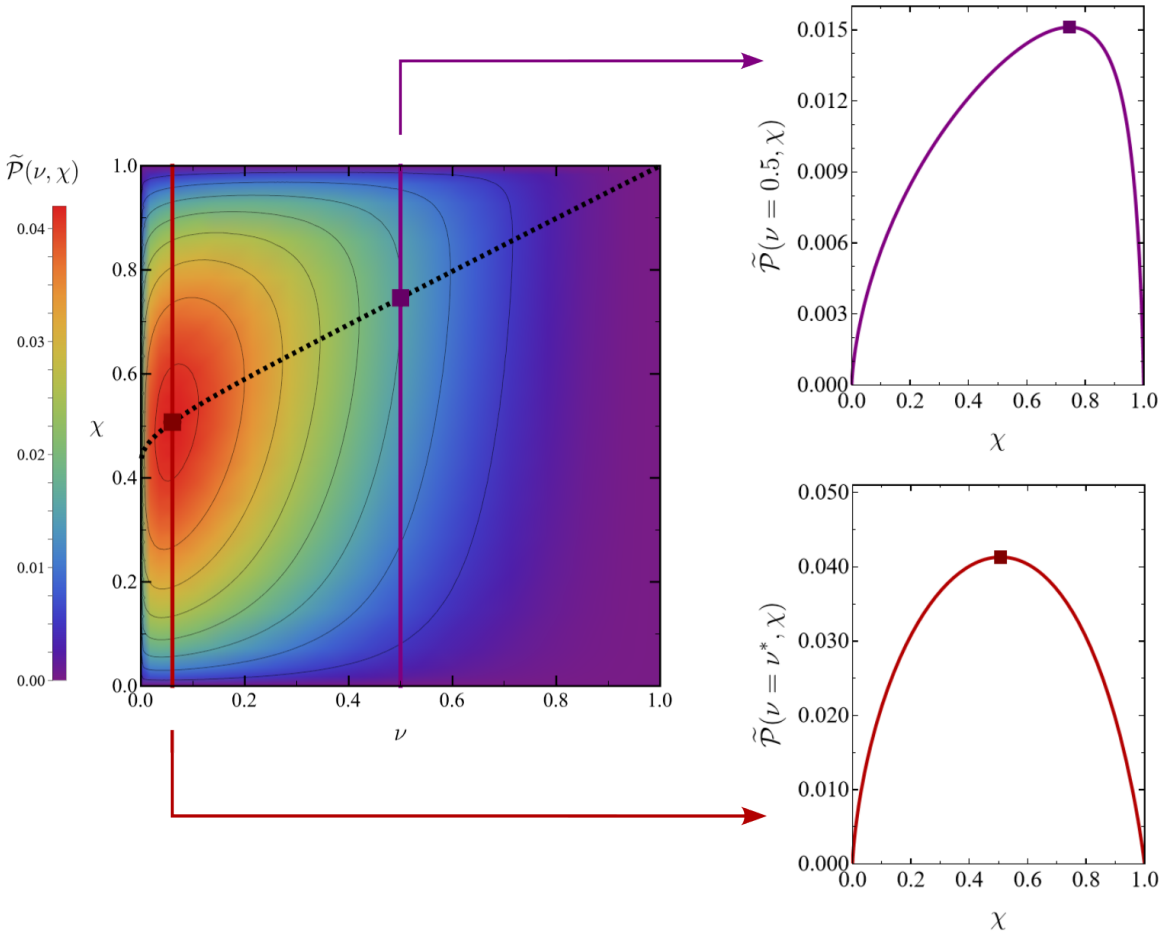


**Figure 4.4:** Density plot of the optimal power in the $(\nu,\chi)$ plane (left) and vertical sections for fixed values of the temperature ratio $\nu$ (right). The curve $\chi = \chi^*(\nu)$ (dotted line) gives the compression ratio yielding optimal power for every temperature ratio. On the right, the upper panel corresponds to $\nu = 0.5$ and the bottom one to $\nu = \nu^*$. The points at which maximum power is reached in each case are also displayed (squares).

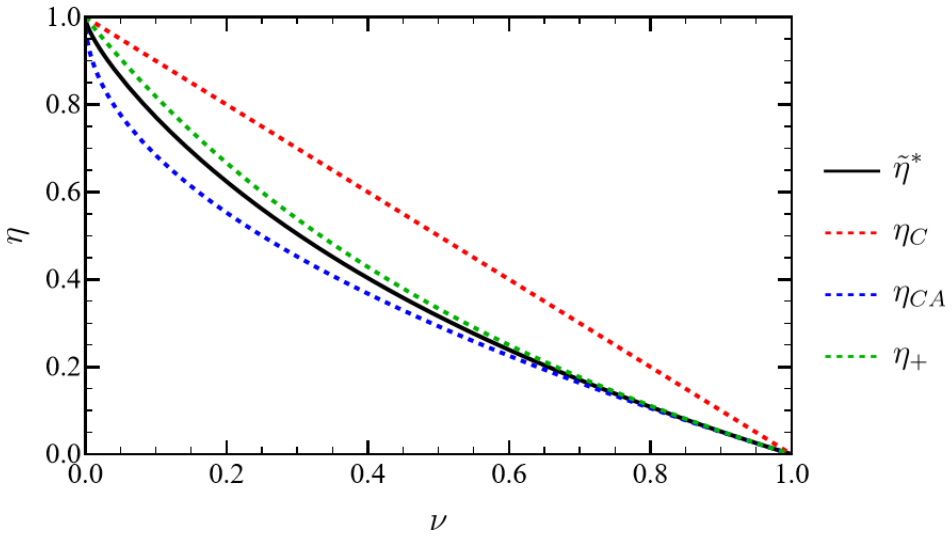


**Figure 4.5:** Efficiency at maximum power in the present approach (black line), Carnot efficiency (red dashed line), Curzon-Ahlborn efficiency (blue dashed line) and $\eta_+$ (green dashed line), defined in Eq. (4.42), as a function of the temperature ratio $\nu$.

In the previous section, we proved that the efficiency of our device is always below the Carnot efficiency, as expected, but above the Curzon-Ahlborn value. Of course, these bounds, which were obtained for arbitrary values of the temperature and compression ratios $(\nu, \chi)$, also apply when optimisation over $\chi$ is carried out,

$$\eta_{CA} < \tilde{\eta}^* < \eta_C. \tag{4.41}$$

This behaviour is illustrated in Fig. 4.5. In addition, we observe that the upper bound of the efficiency at low dissipation

$$\eta_+ \equiv \frac{\eta_C}{2 - \eta_C} = \frac{1 - \nu}{1 + \nu} \tag{4.42}$$

presented in Ref. [22] for engines reaching the Carnot efficiency in the reversible limit, as our Stirling cycle does, is verified in our system.

We are interested in the asymptotic study of the efficiency at maximum power $\tilde{\eta}^*$ in the limit $\nu \to 1$, which corresponds to $\eta_C << 1$. Our approach is the following: we find the expansion of $\chi^*$ in powers of the Carnot efficiency $\eta_C$ and introduce this scaling of $\chi^*$ in $\tilde{\eta}^*(\nu) = \tilde{\eta}(\nu, \chi^*(\nu))$ to obtain the power expansion of $\tilde{\eta}^*$ up to the desired order in $\eta_C$. Thus, let us consider the following ansatz for $\chi^*$ in the limit as $\nu \to 1$:

$$\chi^* = 1 + a_1\,\eta_C + a_2\,\eta_C^2 + a_3\,\eta_C^3 + O\left(\eta_C^4\right), \tag{4.43}$$

where the coefficients $(a_1, a_2, a_3)$ are determined by enforcing the first three terms in the

expansion of the partial derivative of the optimal power with respect to the compression ratio $\partial\widetilde{\mathcal{P}}/\partial\chi$ to vanish at $\chi^*$, since it corresponds to the optimal power output. Note that we determine the zero-order value of $\chi^*$ by using that $\chi^* \to 1$ as $\nu \to 1$, as the dotted line in Fig. 4.4 shows. The described procedure yields

$$a_1 = -\frac{1}{2}, \quad a_2 = -\frac{1}{48}, \quad a_3 = \frac{11}{1152}. \tag{4.44}$$

In Fig. 4.6, we compare the numerically evaluated optimal values of $\chi^*$ with the obtained expansion up to third order in $\eta_C$. The agreement of the numerical solutions and the theoretical estimation is quite good, even when considering a range of $\eta_C$ not so close to zero.

We now introduce the obtained expansion for $\chi^*$ in $\tilde{\eta}^*(\nu) \equiv \tilde{\eta}\left(\nu, \chi^*(\nu)\right)$, obtaining the corresponding expansion for the efficiency,

$$\tilde{\eta}^* = \frac{\eta_C}{2} + \frac{3}{16}\eta_C^2 + \frac{41}{384}\eta_C^3 + O\left(\eta_C^4\right). \tag{4.45}$$

Note that the linear coefficient 1/2 has been proved to be a general upper bound for the linear response at maximum power, as a result of the Onsager reciprocity theorem, which has been considered as the fourth law of thermodynamics [23].

For the Curzon-Ahlborn efficiency, one has

$$\eta_{CA} = \frac{\eta_C}{2} + \frac{\eta_C^2}{8} + \frac{\eta_C^3}{16} + O\left(\eta_C^4\right). \tag{4.46}$$

As expected, we find that the efficiency at maximum power for our engine coincides with the Curzon-Ahlborn efficiency to first order in $\eta_C$. Notwithstanding, the non-linear terms deviate from the Curzon-Ahlborn value. This is not surprising either, since we have proved in the previous section that our efficiency is always above the Curzon-Ahlborn bound, even for arbitrary values of the temperature control bounds $(\theta_{\min}, \theta_{\max})$. It has been shown that the quadratic coefficient being equal to 1/8 is associated with left-right symmetry in the system [21]. It would be interesting to study the role of the asymmetry between heating and cooling processes, triggered by the upper and lower bounds of the temperature control in the isochoric branches of the cycle, on the observed deviation from the Curzon-Ahlborn efficiency yet in second order.

We recall that the expansion of the upper bound $\eta_+$ is

$$\eta_+ = \frac{\eta_C}{2} + \frac{\eta_C^2}{4} + \frac{\eta_C^3}{8} + O\left(\eta_C^4\right). \tag{4.47}$$

This efficiency bound, presented in Ref. [22], is reached in a completely asymmetric limit. Note that the quadratic coefficient in the expansion of our efficiency at optimal power, given in Eq. (4.45), lies between the corresponding values for $\eta_{CA}$ and $\eta_+$: $1/8 < 3/16 < 1/4$.

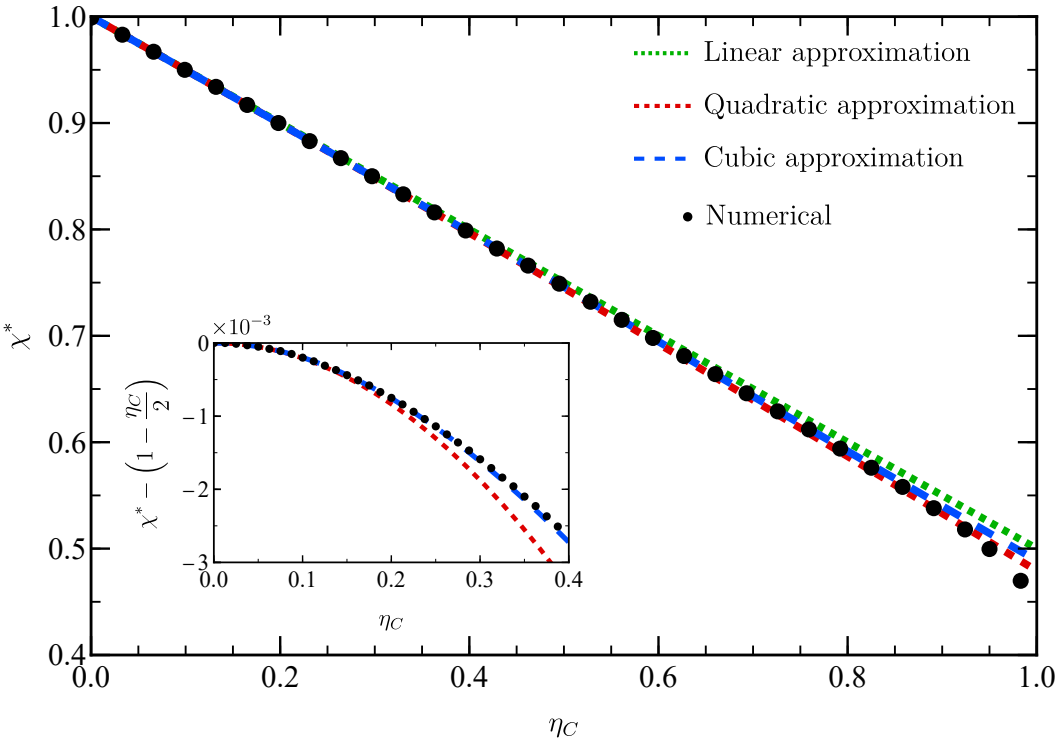


**Figure 4.6:** Optimal compression ratio $\chi^*$ as a function of the corresponding Carnot efficiency $\eta_C = 1 - \nu$. We compare numerical results (black circles) with the perturbative expansion in $\eta_C$ up to linear order (green dotted line), quadratic order (red dashed line) and cubic order (blue dashed line). The inset shows a comparison beyond first order.

#### 4.2.1.2 Optimisation of the irreversible Stirling cycle for variable ($\theta_{\min}$, $\theta_{\max}$)

In this section, we study again the maximisation of the optimal power with respect to the compression ratio $\chi$, but now considering arbitrary bounds $(\theta_{\min}, \theta_{\max})$ in the temperature control. Restrictions concerning these parameters and the temperatures of the cold and hot branches of the cycle arise,

$$\theta_{\min} < \theta_c = \nu < \theta_h = 1 < \theta_{\max}. \tag{4.48}$$

As one may intuitively expect, the most beneficial scenario corresponds to the ideal bounds studied in the previous section: $\theta_{\min} \to 0^+$, $\theta_{\max} \to \infty$. To illustrate how more realistic bounds for the thermal control impinge on the optimal power, we present in Fig. 4.7 the behaviour of $\widetilde{\mathcal{P}}$ as a function of $\chi$ for multiple finite values in one of the bounds (lower or upper) when the other one (upper or lower) reaches the corresponding ideal limit ($\infty$ or 0). We do so for two meaningful values of the temperature ratio: $\nu \in \left\{1/2, \nu^*_{\mathrm{id}}\right\}$, where $\nu^*_{\mathrm{id}}$ denotes the temperature ratio yielding the overall maximum power in the ideal limit

$\theta_{\min} \to 0^+$, $\theta_{\max} \to \infty$ (note that, in the previous section, this parameter was simply written as $\nu^*$).

We observe that, indeed, the optimal power for the ideal bounds $\theta_{\min} \to 0^+$, $\theta_{\max} \to \infty$ is always above the corresponding value for more realistic limits in the thermal control. In addition, the optimal power vanishes when the compression ratio reaches its bounds $\chi \to 0^+$ and $\chi \to 1^-$ in all the studied cases. Hence, there exists an optimal compression ratio $\chi^*$ for each temperature ratio $\nu$ and thermal bounds $(\theta_{\min}, \theta_{\max})$ yielding maximal power. We address this further optimisation of $\widetilde{\mathcal{P}}(\nu, \chi; \theta_{\min}, \theta_{\max})$, given in Eq. (4.32), over the compression ratio $\chi$,

$$\widetilde{\mathcal{P}}^*(\nu; \theta_{\min}, \theta_{\max}) \equiv \max_{\chi \in (0,1)} \widetilde{\mathcal{P}}(\nu, \chi; \theta_{\min}, \theta_{\max}) = \widetilde{\mathcal{P}}(\nu, \chi^*; \theta_{\min}, \theta_{\max}), \tag{4.49}$$

obtaining the maximal power as a function of the temperature ratio in our cycle and the bounds in the thermal control. The associated compression ratio is defined consistently and it also depends on these three parameters, $\chi^* = \chi^*(\nu; \theta_{\min}, \theta_{\max})$.

Similarly to our study of the overall maximal power found in the case of ideal thermal bounds, it is interesting to carry out an even further optimisation over the temperature ratio $\nu$. The interest of such search is transparent: since our physical system is solely submitted to the technical constraints represented by $(\theta_{\min}, \theta_{\max})$, it is natural to wonder what choice of the parameters defining the cycle $(\nu, \chi)$ gives optimal power,

$$\widetilde{\mathcal{P}}^{**}(\theta_{\min}, \theta_{\max}) \equiv \max_{\substack{\chi \in (0,1) \\ \nu \in (\theta_{\min}, 1)}} \widetilde{\mathcal{P}}(\nu, \chi; \theta_{\min}, \theta_{\max}) = \max_{\nu \in (\theta_{\min}, 1)} \widetilde{\mathcal{P}}^*(\nu; \theta_{\min}, \theta_{\max}). \tag{4.50}$$

The optimal parameters are denoted consistently,

$$\nu^* = \nu^*(\theta_{\min}, \theta_{\max}), \qquad \chi^{**}(\theta_{\min}, \theta_{\max}) \equiv \chi^*(\nu^*; \theta_{\min}, \theta_{\max}), \tag{4.51}$$

as well as the corresponding efficiency,

$$\tilde{\eta}^{**}(\theta_{\min}, \theta_{\max}) \equiv \tilde{\eta}(\nu^*, \chi^{**}; \theta_{\min}, \theta_{\max}), \tag{4.52}$$

which are all function of the temperature bounds in the control.

The identification of the optimal parameters $(\nu^*, \chi^{**})$ defining the Stirling cycle over the parallelogram defined by the restrictions $0 < \theta_{\min} < 0.4$ and $1.15 < \theta_{\max} < 2.50$ has been numerically obtained. It is shown, along with the corresponding evaluation of the maximal power $\widetilde{\mathcal{P}}^{**}$ and efficiency $\tilde{\eta}^{**}$, in Fig. 4.8.

As expressed by Eq. (4.37), the efficiency of our engine is always above the Curzon-Ahlborn value. This result, particularised for the overall optimal cycle for fixed $(\theta_{\min}, \theta_{\max})$, is shown in Fig. 4.9. Therein, we present a density plot of $\tilde{\eta}^{**}/\eta_{CA}$ on the above men-

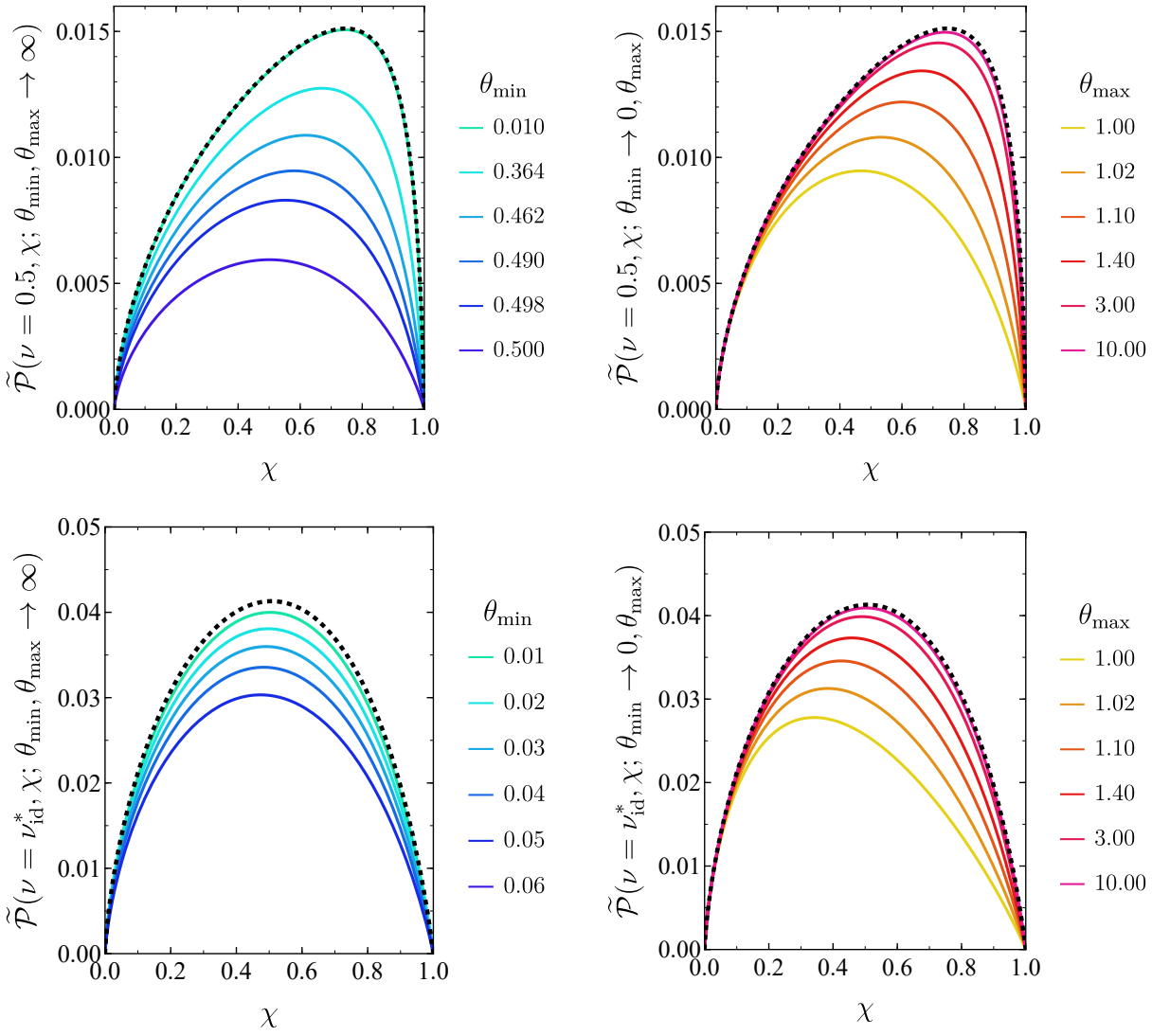


**Figure 4.7:** Optimal power $\widetilde{\mathcal{P}}$ versus the compression ratio $\chi$ for fixed temperature ratios, $\nu = 0.5$ (top panels) and $\nu = \nu^*_{\rm id}$ (bottom panels). In the left (right) panels, the upper (lower) bound in the temperature control reaches its ideal limit, and multiple values of the lower (upper) bound are considered. The optimal power corresponding to the ideal limits of both bounds are also displayed in the four panels (dotted black line).

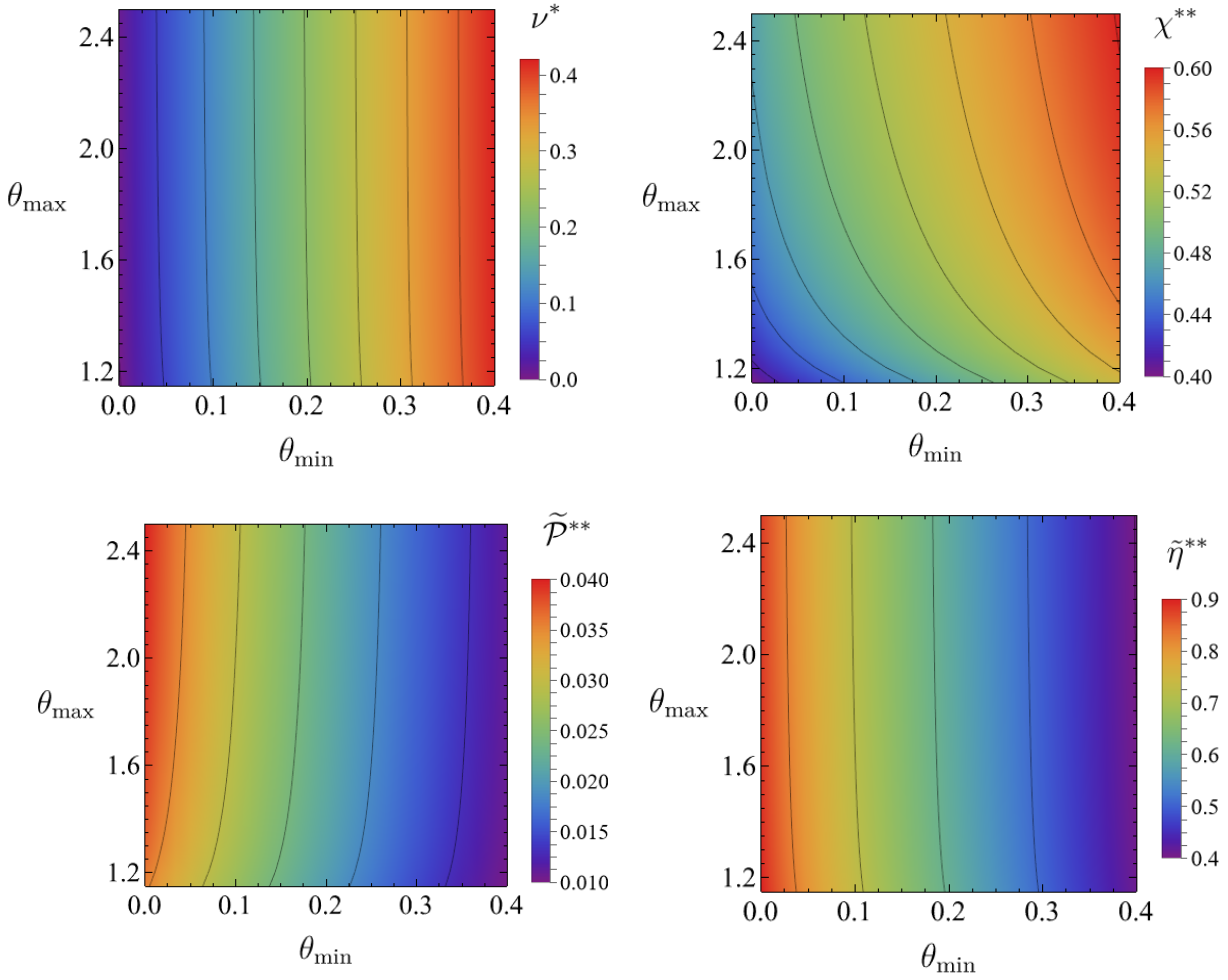


**Figure 4.8:** Density plots of the temperature and compression ratios (top panels) yielding optimal power (bottom left panel), and the corresponding efficiency (bottom right panel) in the $(\theta_{\min}, \theta_{\max})$ plane. We have considered the region defined by intervals $0 < \theta_{\min} < 0.4$, $1.15 < \theta_{\max} < 2.50$.

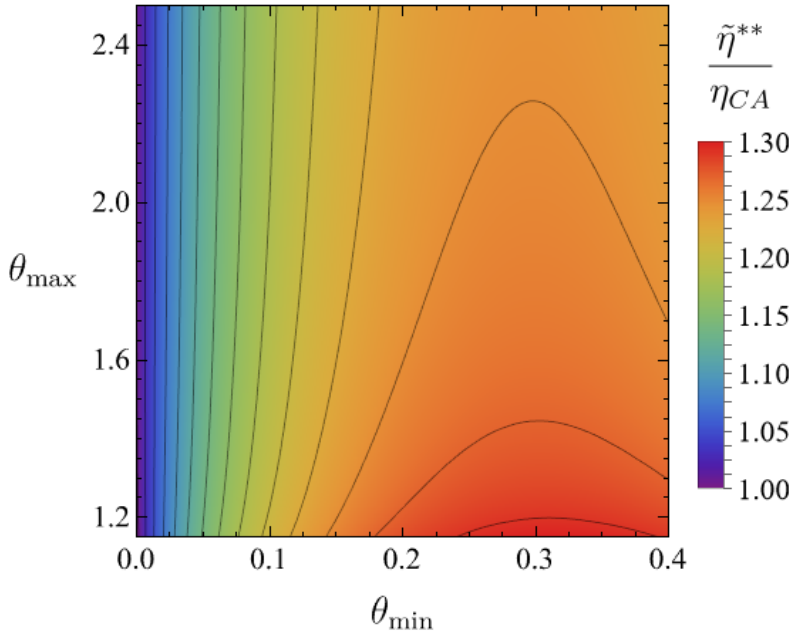


**Figure 4.9:** Density plot of the quotient $\tilde{\eta}^{**}/\eta_{CA}$ in the $(\theta_{\min}, \theta_{\max})$ plane. Similarly to Fig. 4.8, we have considered the region defined by intervals $0 < \theta_{\min} < 0.4$ and $1.15 < \theta_{\max} < 2.50$.

tioned parallelogram in the $(\theta_{\min}, \theta_{\max})$ plane. As theoretically predicted, we observe that the quotient $\tilde{\eta}^{**}/\eta_{CA}$ is always greater than 1. We recall that here the Curzon-Ahlborn efficiency depends on the considered point, since it is given by $\eta_{CA} = 1 - \sqrt{\nu^*}$, and the temperature ratio yielding optimal power depends on the bounds on the thermal control, $\nu^* = \nu^*(\theta_{\min}, \theta_{\max})$.

# Chapter 5

# Conclusions

In the present work, we have designed and optimised an irreversible Stirling-like heat engine, modelled by an overdamped Brownian particle trapped in a harmonic potential, achieving the final goal of this project. The motivation of such a goal is presented in Chapter 1, where a general description of the field of stochastic thermodynamics, within which this work is framed, is given. In order to meet our objective, we have followed the steps that we itemise below:

- First, we have described our model system in Chapter 2. It consists of a Brownian particle in a harmonic trap, in the overdamped regime. Not only does a Brownian particle epitomise the stochastic systems of interest in non-equilibrium statistical mechanics, but is also a very sensible model for practical realisations of colloidal heat engines. The harmonic confinement is also both theoretically and experimentally relevant, since, besides of being a paradigmatic potential in physics, the harmonic oscillator describes optical trapping to a very good approximation.

- We have illustrated the equivalence between the Fokker-Planck and the Langevin approaches, pillars of the description of Markovian processes, by studying the evolution of the position of our Brownian particle in both frameworks. We have been able to prove that, if the initial condition is Gaussian, the solution of both equations is also Gaussian for all times. Thanks to this, we have showed that, with a proper choice of the origin in our coordinate system, the evolution of the position distribution is fully depicted by that of its variance.

- We have obtained the average energy of our system as a function of the particle's position variance, which defines the state of the system, and the temperature of the bath and the stiffness of the trap, both of which have been considered as control parameters. Accordingly, we have obtained the average work and heat exchanges associated with any process connecting equilibrium points.

- In Chapter 3, we have studied in depth the isothermal and isochoric branches of which a Stirling cycle is composed. We have considered both the quasi-static limit and the optimal process in each case. As outlined therein, optimisation is essentially different for isothermal and isochoric transitions. In the first case, we have searched for the maximum delivered irreversible work—which is found to be dependent on the time duration of the transition; whereas in the second case, given that the average work vanishes in isochoric processes, we have looked for the minimum connection time, i.e. the brachistochrone. The first problem can be solved with standard methods of variational calculus, but the second one requires tools from optimal control theory. Expounding the calculation details in Appendix A, the optimal protocol in the isochoric branches is found to be of bang-bang type, exclusively depending on the initial and final states and the external bounds $(\theta_{\min}, \theta_{\max})$ to which the temperature control is submitted.

- Our Stirling stochastic heat engine is put forward in Chapter 4, where four operation points are connected by means of the previously studied isothermal and isochoric branches. The cycle is completely characterised by the temperature ratio $\nu$ and the compression ratio $\chi$. Two scenarios are studied: the quasi-static limit, in which the efficiency attains the Carnot bound but the power output is null, and the cycle delivering maximum power. The latter is designed by maximising work in the isothermal branches and minimising time in the isochoric ones. Thus, the optimal delivered power and its corresponding efficiency are obtained for every point on the $(\nu, \chi)$ plane. We have verified that the efficiency at optimal power for our irreversible cycle is always below the Carnot efficiency but, noteworthily, above the Curzon-Ahlborn efficiency.

- A further optimisation has been carried out by finding the optimal compression ratio yielding maximum power for any given temperature ratio. Finally, we have maximised power over the temperature ratio as well. The case of ideal bounds in temperature, $\theta_{\min} \to 0^+$, $\theta_{\max} \to \infty$, has been studied first. Therein, the behaviour of the optimal efficiency in the limit $\nu \to 1^-$ has been asymptotically predicted and compared to representative efficiencies found in the literature. Secondly, arbitrary finite bounds, allowing for a more realistic description of experimental studies, have been considered.

Possible future research work based on the present results are discussed in the following. First, considering an alternative normalisation for the temperatures, taking $\theta_{\max} = 1$, is worth-studying. In practical experiments, the maximum feasible temperature is fixed, whereas the temperature of the hot isotherm $\theta_h$ can be conveniently tuned. The proposed renormalisation permits the study of the limit $\theta_h \to \theta_{\max}^-$ in a more natural manner, even

when the upper bound of the temperature is considered as infinite. Second, it would be especially interesting to implement the proposed engine in practice. Present-day experimental techniques make it possible to control both the stiffness of the trap—using optical tweezers—and the temperature of the bath—which is effectively modified by applying a random electric field whose amplitude is controlled. Experimental realisations of micrometre-sized stochastic Stirling engines have already been presented in the literature [15]. Third, investigating the irreversible analogue of other classical thermodynamic cycles, such as Otto's or Diesel's, may lead to interesting results, both on the theoretical and experimental contexts. Finally, it would be interesting to analyse the fluctuations of the relevant magnitudes in our irreversible Stirling cycle, obtaining a deeper theoretical characterisation of the heat engine, beyond the mean values considered in the present work.

# Bibliography


[1] H. B. Callen, *Thermodynamics and an Introduction to Thermostatistics*, (Wiley, 1985).

[2] U. Seifert, Reports on Progress in Physics **75**, 126001 (2012).

[3] I. A. Martínez, E. Roldán, L. Dinis, and R. A. Rica, Soft Matter **13**, 22 (2017).

[4] C. A. Plata, D. Guéry-Odelin, E. Trizac, and A. Prados, Physical Review E **101**, 032129 (2020).

[5] W. Thomson, Nature **20**, 126 (1879).

[6] S. Ciliberto, Physical Review X **7**, 021051 (2017).

[7] E. Lutz and S. Ciliberto, Physics Today **68**, 30 (2015).

[8] T. Schmiedl and U. Seifert, Physical Review Letters **98**, 108301 (2007).

[9] A. Patrón, A. Prados, and C. A. Plata, The European Physical Journal Plus **137**, 1011 (2022).

[10] I. A. Martínez, A. Petrosyan, D. Guéry-Odelin, E. Trizac, and S. Ciliberto, Nature Physics **12**, 843 (2016).

[11] D. Guéry-Odelin, C. Jarzynski, C. A. Plata, A. Prados, and E. Trizac, Reports on Progress in Physics **86**, 035902 (2023).

[12] T. Schmiedl and U. Seifert, EPL (Europhysics Letters) **81**, 20003 (2008).

[13] I. Martínez, E. Roldán, L. Dinis, D. Petrov, J. M. Parrondo, and R. Rica, Nature Physics **12**, 67 (2015).

[14] C. A. Plata, D. Guéry-Odelin, E. Trizac, and A. Prados, Journal of Statistical Mechanics: Theory and Experiment 093207 (2020).

[15] V. Blickle and C. Bechinger, Nature Physics **8**, 143 (2012).

[16] I. Tlili, Renewable and Sustainable Energy Reviews **16**, 2234 (2012).

[17] N. G. Van Kampen, *Stochastic Processes in Physics and Chemistry*, (Elsevier, 1992).

[18] C. W. Gardiner, *Handbook of Stochastic Methods for Physics, Chemistry and the Natural Sciences*, (Springer, 1985).

[19] Y. Band, O. Kafri, and P. Salamon, Journal of Applied Physics **53**, 8 (1982).

[20] F. L. Curzon and B. Ahlborn, American Journal of Physics **43**, 22 (1975).

[21] M. Esposito, K. Lindenberg, and C. Van den Broeck, Physical Review Letters **102**, 130602 (2009).

[22] M. Esposito, R. Kawai, K. Lindenberg, and C. Van den Broeck, Physical Review Letters **105**, 150603 (2010).

[23] C. Van den Broeck, Physical Review Letters **95**, 190602 (2005).

[24] L. S. Pontryagin, *Mathematical Theory of Optimal Processes*, (CRC Press, 1987).

[25] D. Liberzon, *Calculus of Variations and Optimal Control Theory: A Concise Introduction*, (Princeton University Press, 2012).

# Appendix A

# Pontryagin's Maximum Principle

Pontryagin's Maximum Principle provides the convenient mathematical tool for the bounded optimisation problem that we have stated in Sec. 3.2.2 [24]. In the following, we enunciate the general time-optimal problem undertaken by a particularisation of Pontryagin's Principle and later we focus on the one-dimensional case concerning our isochoric branches.

## A.1 Pontryagin's Time-Optimal Problem

**Statement of the Pontryagin's Time-Optimal Problem** Let us consider an object whose law of motion can be written in the form of a system of differential equations

$$\frac{dx^i}{dt} = f^i(x^1, \dots x^n, u^1, \dots, u^r) \equiv f^i(\boldsymbol{x}, \boldsymbol{u}), \quad i = 1, \dots, n, \tag{A.1}$$

which are equivalent to the differential vector equation

$$\frac{d\boldsymbol{x}}{dt} = \big(f^1(\boldsymbol{x}, \boldsymbol{u}), \dots, f^n(\boldsymbol{x}, \boldsymbol{u})\big) \equiv \boldsymbol{f}(\boldsymbol{x}, \boldsymbol{u}). \tag{A.2}$$

Here, $\boldsymbol{x} \equiv (x^1, \dots, x^n)$ are the phase coordinates of the system, belonging to the phase space $X$; $\boldsymbol{u} \equiv (u^1, \dots, u^r)$ are the control parameters, which determine the course of the process and belong to a 'control region' $U$; $t$ denotes time; and $f^i : X \times U \to \mathbb{R}$ are continuous functions which are also differentiable with respect to the phase coordinates.

Arbitrary piecewise continuous controls $\boldsymbol{u} = \boldsymbol{u}(t)$ are admissible. Thence, for any control function, defined on an interval $[t_0, t_f]$, there exists, at most, a finite number $k$ of time instants $\alpha_0 \equiv t_0 < \alpha_1 < \ldots < \alpha_k < \alpha_{k+1} \equiv t_f$ at which the control may have finite jump discontinuities (an example is shown in the top panel of Fig. A.1).

For any given control $\boldsymbol{u} = \boldsymbol{u}(t)$ and any chosen initial condition $\boldsymbol{x}(t_0) = \boldsymbol{x}_0$, in most cases it is possible to uniquely define the evolution of the system $\boldsymbol{x}(t)$ in phase space to be continuous and piecewise differentiable (see Fig. A.1). The procedure that allows

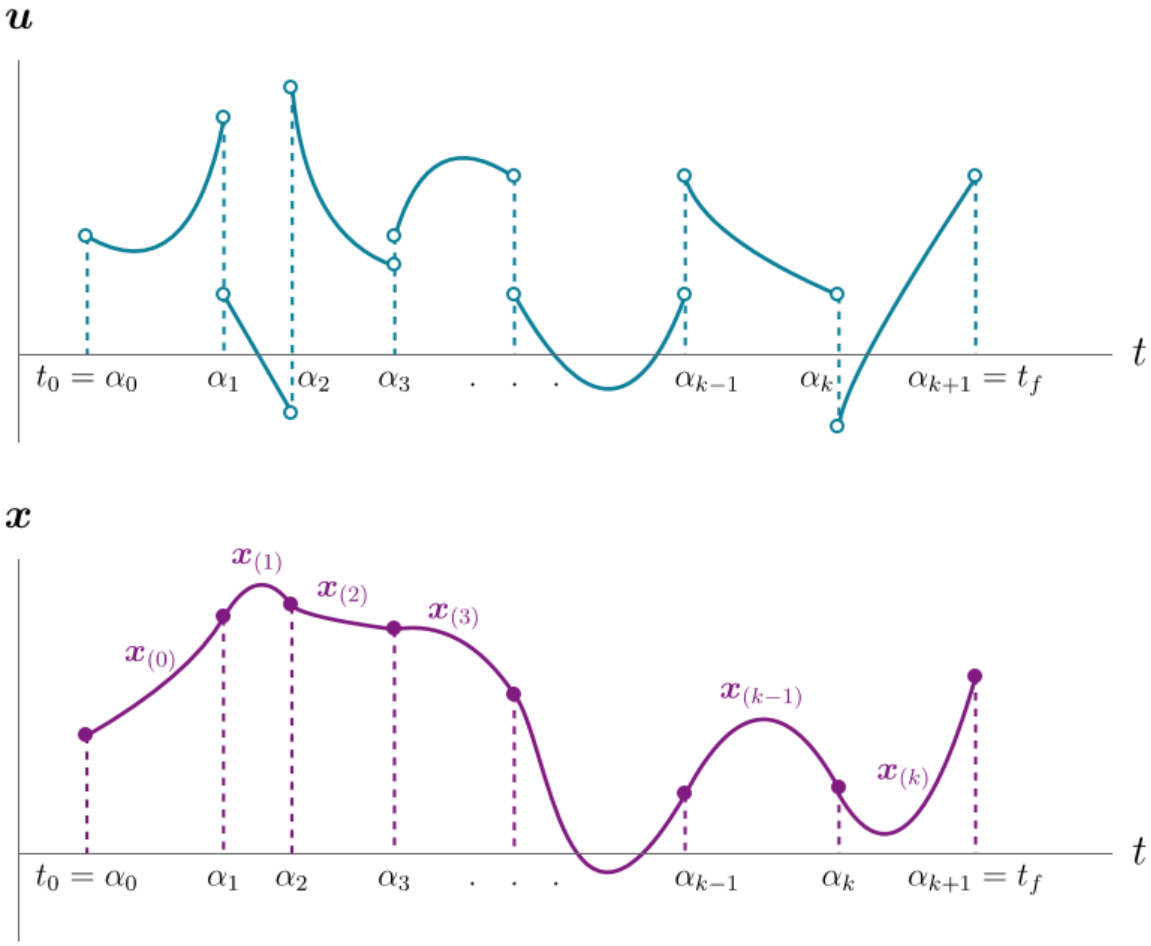


**Figure A.1:** Qualitative representation of the control $\boldsymbol{u}$ (top panel) and the corresponding phase coordinate $\boldsymbol{x}$ (bottom panel) time evolutions. For the sake of clarity, we have considered one-dimensional variables in both cases.

for the construction of such function consists in concatenating the solutions of the initial value problems associated with the system in Eq. (A.1) (or, equivalently, Eq. (A.2)) and appropriate initial conditions for each interval in which the control $\boldsymbol{u}(t)$ is continuous.[1] Namely, the first initial value problem that we need to consider is

$$\begin{cases} \dfrac{d\boldsymbol{x}}{dt} = \boldsymbol{f}(\boldsymbol{x}, \boldsymbol{u}(t)), \quad \alpha_0 \leq t \leq \alpha_1, \\ \boldsymbol{x}(\alpha_0) = \boldsymbol{x}_0. \end{cases} \tag{A.3}$$

Let us denote as $\boldsymbol{x}_{(0)}(t)$ the solution of problem stated in Eq. (A.3), whose existence is assumed. Subsequently, we need to solve the initial value problems

$$\begin{cases} \dfrac{d\boldsymbol{x}}{dt} = \boldsymbol{f}(\boldsymbol{x}, \boldsymbol{u}(t)), \quad \alpha_j \leq t \leq \alpha_{j+1}, \\ \boldsymbol{x}(\alpha_j) = \boldsymbol{x}_{(j-1)}(\alpha_j). \end{cases} \qquad j = 1, \ldots, k, \tag{A.4}$$

where $\boldsymbol{x}_{(j)}(t)$ is the solution corresponding to the $j$-th interval (i.e. $[\alpha_j, \alpha_{j+1}]$ for $j = 0, \ldots, k$), which, again, is assumed to exist. The chosen initial condition in Eq. (A.4) guarantees the continuity of the constructed solution, which is said to *correspond* to the control $\boldsymbol{u}(t)$, and it is given by the following expression,

$$\boldsymbol{x}(t) = \boldsymbol{x}_{(j)}(t), \quad \alpha_j \leq t \leq \alpha_{j+1}; \quad \forall j = 0, \ldots k. \tag{A.5}$$

If the obtained solution $\boldsymbol{x}(t)$ satisfies the additional boundary condition $\boldsymbol{x}(\alpha_{k+1}) = \boldsymbol{x}_f$, we shall say that the considered control $\boldsymbol{u}(t)$ *transfers* the phase point from the position $\boldsymbol{x}_0$ to the position $\boldsymbol{x}_f$. Now, we are ready to formulate the optimisation problem that we need to assess:

*Given two points $\boldsymbol{x}_0, \boldsymbol{x}_f \in X$, we aim to find, among the admissible controls $\boldsymbol{u}(t)$ which transfer the phase point from position $\boldsymbol{x}_0$ to $\boldsymbol{x}_f$ (if such controls exist), one for which the functional*

$$J[\boldsymbol{u}] = \int_{t_0}^{t_f} dt = t_f - t_0 \tag{A.6}$$

*attains its minimum possible value.*

**Maximum Principle for Time-Optimal Processes** Pontryagin's Maximum Principle provides a necessary condition for optimality. It can be applied to a wider range of problems in which, instead of the functional given in Eq. (A.6), more general ones with

[1] We extend the definition intervals for the studied initial value problems to be closed ones, considering the corresponding limit values for the control $\boldsymbol{u}(t)$, which is not strictly defined on the endpoints $\alpha_j$.

explicit dependence on the control $\boldsymbol{u}(t)$ and the phase-space trajectory $\boldsymbol{x}(t)$ are covered. The proof of the Maximum Principle and its general formulation go beyond the purposes of this text and they are omitted, but can be found in Refs. [24, 25].

In the case of the Time-Optimal Problem previously formulated, we shall consider an additional system of equations in the auxiliary variables $\boldsymbol{\psi} \equiv (\psi_1, \ldots, \psi_n)$,

$$\frac{d\psi_i}{dt} = -\sum_{\alpha=1}^{n} \frac{\partial f^\alpha(\boldsymbol{x}, \boldsymbol{u})}{\partial x^i} \psi_\alpha, \quad i = 1, \ldots, n. \tag{A.7}$$

For a given control $\boldsymbol{u}(t)$ and the corresponding trajectory $\boldsymbol{x}(t)$, this system becomes linear and homogeneous, and thus it has a uniquely defined solution $\boldsymbol{\psi}(t)$. For clarity, this solution is said to *correspond* to the chosen control evolution $\boldsymbol{u}(t)$ and phase trajectory $\boldsymbol{x}(t)$.

**Theorem 1** (Necessary Condition for Time-Optimality)**.** *If the control $\boldsymbol{u}(t)$ and the corresponding trajectory $\boldsymbol{x}(t)$ are time-optimal, then there exists a continuous, nonzero vector function $\boldsymbol{\psi}(t)$ corresponding to them which verifies the following conditions:*

1. *The so-called 'Pontryagin's Hamiltonian', defined as*

$$H(\boldsymbol{\psi}(t), \boldsymbol{x}(t), \boldsymbol{u}(t)) \equiv \sum_{i=1}^{n} \psi_n f^n(\boldsymbol{x}(t), \boldsymbol{u}(t)), \tag{A.8}$$

*reaches its maximum value*

$$M(\boldsymbol{\psi}, \boldsymbol{x}) = \sup_{u \in U} H(\boldsymbol{\psi}, \boldsymbol{x}, \boldsymbol{u}) \tag{A.9}$$

*for all $t \in [t_0, t_f]$,*

$$H(\boldsymbol{\psi}(t), \boldsymbol{x}(t), \boldsymbol{u}(t)) = M(\boldsymbol{\psi}(t), \boldsymbol{x}(t)), \quad \forall t \in [t_0, t_f]\,. \tag{A.10}$$

2. *Pontryagin's Hamiltonian is non-negative at the terminal time:*

$$M(\boldsymbol{\psi}(t_f), \boldsymbol{x}(t_f)) \geq 0. \tag{A.11}$$

*Furthermore, if Eq.* (A.10) *is verified, the function $M$ is found to be constant in time. Thus, condition in Eq.* (A.11) *can be equivalently stated $\forall t \in [t_0, t_f]$, not only at the terminal time $t_f$.*

In general, existence and sufficiency conditions for optimality are difficult to find and exhibit a strong dependence on the vector function $\boldsymbol{f}(\boldsymbol{x}, \boldsymbol{u})$ characterising the evolution of the trajectory in the phase space. Fortunately, in our case of interest this function is

linear in its variables and this yields interesting and useful properties. In particular, the existence of an optimal control is guaranteed.

Note that, with the definition of $H$ given in Eq. (A.8), the systems in Eqs. (A.1) and (A.7) are equivalent to

$$\begin{cases} \dfrac{dx^i}{dt} = \dfrac{\partial H}{\partial \psi_i}, & i = 1, \dots, n, \\ \dfrac{d\psi_i}{dt} = -\dfrac{\partial H}{\partial x^i}, & i = 1, \dots, n. \end{cases} \tag{A.12}$$

**Linear Time-Optimal Processes** Let us now consider the case in which functions describing the trajectory evolution in the phase space are linear:

$$f^i(\boldsymbol{x}, \boldsymbol{u}) = \sum_{\mu=1}^{n} a^i_\mu x^\mu + \sum_{\nu=1}^{r} b^i_\nu u^\nu, \quad i = 1, \dots, n, \tag{A.13}$$

or, in vector form,

$$\boldsymbol{f}(\boldsymbol{x}, \boldsymbol{u}) = A\boldsymbol{x} + B\boldsymbol{u}, \tag{A.14}$$

where $A$ and $B$ are linear operators defined, respectively, by matrices $(a^i_\mu)$ and $(b^i_\nu)$. Furthermore, in this case we shall consider the control region $U$ to be a parallelepiped verifying that every vector $\boldsymbol{v} \in U$ with the direction of one of its edges satisfies that

$$B\boldsymbol{v},\ AB\boldsymbol{v}, \dots\ A^{n-1}B\boldsymbol{v} \tag{A.15}$$

are linearly independent.

In this particular case, Pontryagin's Hamiltonian takes de form

$$H(\boldsymbol{\psi}, \boldsymbol{x}, \boldsymbol{u}) = (\boldsymbol{\psi}, A\boldsymbol{x}) + (\boldsymbol{\psi}, B\boldsymbol{u}) = \sum_{i,\mu} \psi_i a^i_\mu x^\mu + \sum_{i,\nu} \psi_i b^i_\nu u^\nu, \tag{A.16}$$

where $(\cdot\,,\cdot)$ denotes the scalar product. In this particular case of study, the second equality in Eq. (A.12) can be written as

$$\frac{d\psi_i}{dt} = -\frac{\partial H}{\partial x^i} = -\sum_{j=1}^{n} a^j_i \psi_j, \quad i = 1, \dots, n; \tag{A.17}$$

or, equivalently, in vector form,

$$\frac{d\boldsymbol{\psi}}{dt} = -A^T\boldsymbol{\psi}. \tag{A.18}$$

Theorem 1 implies that, if $\boldsymbol{u}(t)$ is an optimal control transfering the phase point from $\boldsymbol{x}_0$ to $\boldsymbol{x}_f$, there must exist a solution $\boldsymbol{\psi}(t)$ of Eq. (A.18) verifying Eq. (A.10). In particular, as the first term in Eq. (A.16) does not depend explicitly on the control, the optimal

solution $\tilde{\boldsymbol{u}}$ satisfies that

$$P(\boldsymbol{\psi}(t)) \equiv \sup_{u\in U} (\boldsymbol{\psi}(t), B\boldsymbol{u}(t)) = (\boldsymbol{\psi}(t), B\tilde{\boldsymbol{u}}(t)) \,. \tag{A.19}$$

Note that, for any given solution $\boldsymbol{\psi}(t)$ of system in Eq. (A.17), this equation can be used to determine possible optimal controls $u(t)$. Is condition in Eq. (A.19) sufficient for determining the control uniquely? The next theorem (whose proof may be consulted in Ref. [24]) yields an answer for this question.

**Theorem 2.** *If all the eigenvalues of matrix $A$ are real, then, for every non-trivial solution $\boldsymbol{\psi}(t)$ of Eq.* (A.18) *(or, equivalently, system in Eq.* (A.17)*), relation in Eq.* (A.19) *uniquely determines the control function. Moreover, each component $u^j(t)$, $= 1, \dots r$ is piecewise constant, taking on only the minimum and maximum values of the interval in which it is bounded, and it has at most $n-1$ jump discontinuities. Hence, the control is a so-called 'bang-bang' protocol.*

## A.2 Thermal brachistochrone for an isochoric branch

We now return to our particular system of interest: a one-dimensional harmonically confined Brownian particle in an isochoric process. The application of Pontryagin's Maximum Principle is extremely simple in this special case.

We aim to minimise the functional

$$J\,[\theta] = \int_0^{\tau_f} d\tau = \tau_f, \tag{A.20}$$

which corresponds to the duration of the process.

We start by recalling that our phase space is three-dimensional, with the state of the system being determined by the triplet $(\kappa, y, \theta)$. Since we are in an isochoric branch, $\kappa$ is fixed and the temperature $\theta$ is considered as the control. Accordingly, our 'effective' phase space in this case is one-dimensional ($n = 1$) and it is characterised by a single coordinate $x^1 = y$. Likewise, the control region is also one-dimensional ($r = 1$), since the only control considered is the temperature $u^1 = \theta$. Furthermore, it is bounded on a closed interval: $\theta_{\min} \leq \theta \leq \theta_{\max}$, which corresponds to the one-dimensional version of a parallelepiped. Given that $n = r = 1$, instead of the system in Eq. (A.1), we have a single equation

$$\frac{dy}{d\tau} = f^1(y, \theta) \equiv -2\kappa y + 2\theta. \tag{A.21}$$

It is a linear equation of the form previously studied, with $A = -2\kappa$ and $B = 2$ (note that $A$ and $B$ are scalars here). In this one-dimensional case, condition in Eq. (A.15)

is superfluous (a unitary set is not linearly dependent if and only if its only element is zero, i.e. if $v = 0$, but then $v$ would not determine any direction). Hence, the linearity of Eq. (A.21) and the type of bounds for $\theta$ imply that our problem corresponds to a linear time-optimal process.

Although Theorem 2 proves that the optimal protocol must be constant with either $\theta(t) = \theta_{\max}$ or $\theta(t) = \theta_{\min}$ (this depends on whether we intend to heat or cool our system), we shall derive the result for this simple case.

Pontryagin's Hamiltonian reads

$$H(\psi, y, \theta) = (-2\kappa y + 2\theta)\,\psi. \tag{A.22}$$

Thus, in this case, Eq. (A.18) is written as follows,

$$\frac{d\psi}{d\tau} = -\frac{\partial H}{\partial y} = 2\kappa\psi. \tag{A.23}$$

The general solution for this first-order differential equation is

$$\psi(\tau) = \psi_0 e^{2\kappa\tau}, \tag{A.24}$$

which does not depend on the control parameter $\theta$ and has a well-defined constant sign, dependent on the initial value $\psi_0$. According to our previous discussion, the Hamiltonian attains a maximum at the optimal value, and thence

$$\frac{\partial H}{\partial \theta} = 2\psi = 0 \tag{A.25}$$

if the optimal control belonged to the open interval $\theta(\tau) \in (\theta_{\min}, \theta_{\max})$. Nevertheless, this is not possible, since, as we just mentioned, $\psi$ is either positive or negative in the whole time interval. This is an alternative path to prove that the solution of our problem is a bang-bang protocol without 'switchings' (i.e. with a single continuity interval), in which $\theta(\tau)$ is equal to one of its bounds. In a heating process, we have that $\tilde{\theta}(\tau) = \theta_{\max}$, $\forall\tau \in (0, \tau_f)$, whereas $\tilde{\theta}(\tau) = \theta_{\min}$, $\forall\tau \in (0, \tau_f)$ in a cooling procedure. Thus, the optimal control $\tilde{\theta}(\tau)$, which is illustrated in Fig. A.2, can be expressed as

$$\tilde{\theta}(\tau) = \tilde{\theta} \equiv \begin{cases} \theta_{\max}, & \text{if} \quad \theta_i < \theta_f, \\ \theta_{\min}, & \text{if} \quad \theta_i > \theta_f, \end{cases} \qquad \forall\tau \in (0, \tau_f)\,. \tag{A.26}$$

Note that $\tilde{\theta}(\tau)$ is discontinuous at the initial and final time instants, given that it is submitted to the boundary conditions

$$\tilde{\theta}(0) = \theta_i, \quad \tilde{\theta}(\tau_f) = \theta_f. \tag{A.27}$$

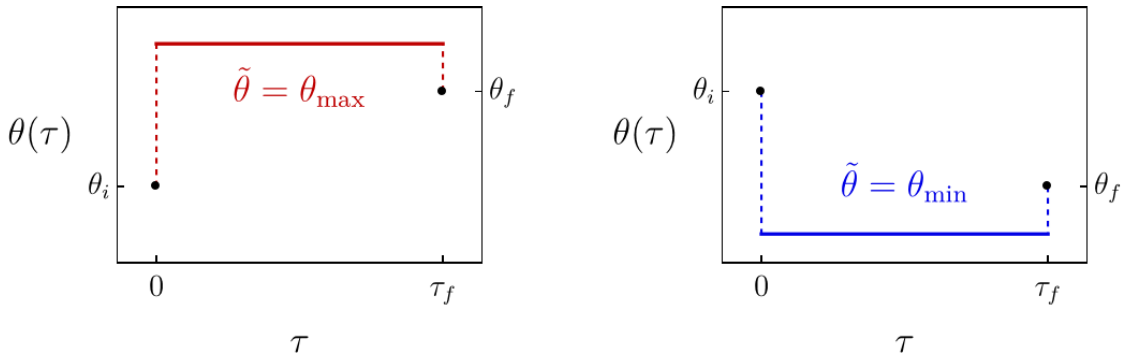


**Figure A.2:** Sketch of the optimal temperature driving in heating (left panel) and cooling (right panel) processes.

# Addendum: Code example

The numerical optimisation problems presented throughout this work have been solved using the software *Mathematica 13.1*. In this addendum, we include the notebook used to find the overall optimum in Sec. 4.2.1.1 as an illustrative example. The codes used to obtain the rest of our results are similar and they are omitted for the sake of conciseness.

## Optimisation of the irreversible Stirling cycle in the limit $\theta_{max} \to \infty,\ \theta_{min} \to 0$

```
In[ ]:= ClearAll["Global`*"]
In[ ]:= << MaTeX`
```

### Definition of physical quantities and parameters

```
In[ ]:= Wqs[ν_, χ_] := (1 - ν)/2 Log[χ];
        α[χ_] := (1/Sqrt[χ] - 1)^2;
        w[ν_, χ_] := -Wqs[ν, χ] / (α[χ] * (1 + Sqrt[ν])^2);
        tisoc[ν_, χ_] := -1/(2 χ) Log[ν];
        σ[ν_, χ_] := Sqrt[1 + w[ν, χ] * tisoc[ν, χ]];
        tAB[ν_, χ_] := (1 + σ[ν, χ]) / (w[ν, χ] * (1 + Sqrt[ν]));
        tCD[ν_, χ_] := Sqrt[ν] * tAB[ν, χ];
        WAB[ν_, χ_] := Log[χ]/2 + α[χ]/tAB[ν, χ];
        WCD[ν_, χ_] := (-ν * Log[χ])/2 + (ν * α[χ])/tCD[ν, χ];
        P[ν_, χ_] :=
          -((WAB[ν, χ] + WCD[ν, χ]) / (tAB[ν, χ] + tCD[ν, χ] + tisoc[ν, χ]));
        η[ν_, χ_] := 1 + WCD[ν, χ]/WAB[ν, χ];
        ηC[ν_] := 1 - ν;
        ηCA[ν_] := 1 - Sqrt[ν];
```

## Optimisation over the compression ratio: $\chi^*(v)$

We search for the compression ratio yielding maximum delivered power for each temperature ratio, using the obtained theoretical expansion of $\chi^*$ up to third order in $\eta_C = 1 - v$ as starting point.

```
pχopt[ν_] := FindMaximum[{P[ν, χ], 0 < χ < 1},
  {χ, 1 - 1/2 (1 - ν) - 1/48 (1 - ν)^2 + 11/1152 (1 - ν)^3}]
popt[ν_] := First[pχopt[ν]]
χopt[ν_] := χ /. Last[pχopt[ν]]
```

This direct approach only gives satisfactory results for $0<v<0.9$ , but the flatness and smallness of the power for $0.9<v<1$ triggers notable numerical error in this interval.

Using a monotonically increasing transformation of the power allows for finding the actual optimal compression ratio in the interval $0.9<v<0.99$. Specifically, we use here the transformation $x \to e^{x+5}$.

```
fχoptAux[ν_] := FindMaximum[{Exp[P[ν, χ] + 5], 0.9 < χ < 1},
  {χ, 1 - 1/2 (1 - ν) - 1/48 (1 - ν)^2 + 11/1152 (1 - ν)^3}]
χoptAux[ν_] := χ /. Last[fχoptAux[ν]]
```

For $v>0.99$, we use a fine mesh for directly obtaining $\chi^*$ by comparing the corresponding delivered power among all the considered values of $\chi$ for every $v$ in the mesh.

```
δ = 10^-6;
xs := Table[x, {x, 0.99, 1 - δ, δ}];
PauxMesh[ν_] := Table[P[ν, x], {x, 0.99, 1 - δ, δ}]
χoptAuxMesh[ν_] := xs[[Ordering[PauxMesh[ν], -1]]][[1]];
```

We perform the described calculations to obtain a table $\{v, \chi^*(v)\}$ and we interpolate in order to estimate $\chi^*(v)$ in the whole interval $0<v<1$.

```
point1 = 0.90;
point2 = 0.99;
Δ = 10^-3;
χsOptA := Table[{N[ν], χopt[ν]}, {ν, Δ, point1 - Δ, Δ}]
χsOptB := Table[{ν, χoptAux[ν]}, {ν, point1, point2 - Δ, Δ}]
χsOptC := Table[{ν, χoptAuxMesh[ν]}, {ν, point2, 1 - Δ, Δ}]
χsOpt := Join[χsOptA, χsOptB, χsOptC]
fχsOpt = Interpolation[χsOpt];
```

## Optimisation over the temperature ratio: $v^*$

```
νopt := ν /. Last[FindMaximum[{P[ν, fχsOpt[ν]], 0 < ν < 1}, {ν, 0.08}]]
```

### Calculation of $\{v^*, \chi^{**}, P(v^*, \chi^{**})\}$

In[ ]:=
```
{νopt, fχsOpt[νopt], P[νopt, fχsOpt[νopt]]}
```

Out[ ]=
```
{0.0604619, 0.507215, 0.0413035}
```

## Figure

```
LTicks[xm_, xM_, ΔxM_, Δxm_, n_] :=
  Join[Table[{x, NumberForm[x, {2, n}],
     {0.02, 0}, Thickness[0.004]}, {x, xm, xM, ΔxM}],
   Table[{x, "", {0.01, 0}, Thickness[0.002]}, {x, xm, xM, Δxm}]];

STicks[xm_, xM_, ΔxM_, Δxm_] :=
  Join[Table[{x, "", {0.02, 0}, Thickness[0.004]}, {x, xm, xM, ΔxM}],
   Table[{x, "", {0.01, 0}, Thickness[0.002]}, {x, xm, xM, Δxm}]];

LTicksLegend[xm_, xM_, ΔxM_, Δxm_, n_] :=
  Join[Table[{x, NumberForm[x, {2, n}],
     {0.02, 0}, Thickness[0.004]}, {x, xm, xM, ΔxM}],
   Table[{x, "", {0.01, 0}, Thickness[0.002]}, {x, xm, xM, Δxm}]];


xm = 0; xM = 1; Δxm = 0.1; ΔxM = 0.2;
ym = 0; yM = 1; Δym = 0.1; ΔyM = 0.2;
min = 0; max = 0.042; step = 0.01;
Colors = "Rainbow"; magnif = 2;
```

```
Show[DensityPlot[P[ν, χ], {ν, xm, xM},
  {χ, ym, yM}, PlotRange → {{xm, xM}, {ym, yM}, {min, max}},
  ColorFunction → ColorData[Colors],
  PlotLegends → BarLegend[{Colors, {min, max}}, Ticks →
     LTicksLegend[min, max, step, step / 2, 2], LegendMarkerSize → 250,
    LegendLabel → MaTeX["\\widetilde{\\mathcal{P}}(\\nu,\\chi)",
      Magnification → magnif], LegendMargins → {{-4, 0}, {35, 0}}],
  LabelStyle → Directive[Black, 16, FontFamily → "Times New Roman"],
  RotateLabel → False, Axes → False,
  FrameStyle → Directive[Black, 20,
    FontFamily → "Times New Roman", Thickness[0.004]],
  FrameLabel → {MaTeX["\\nu", Magnification → magnif],
    MaTeX["\\chi", Magnification → magnif]}, ImageSize → Medium,
  FrameTicks → {{LTicks[ym, yM, ΔyM, Δym, 1], STicks[ym, yM, ΔyM, Δym]},
    {LTicks[xm, xM, ΔxM, Δxm, 1], STicks[xm, xM, ΔxM, Δxm]}},
  PlotRangeClipping → False], ContourPlot[P[ν, χ], {ν, xm, xM},
  {χ, ym, yM}, PlotRange → {{xm, xM}, {ym, yM}, {min, max}},
  Contours → Table[x, {x, min, max, step / 2}], ContourShading → False],
 ParametricPlot[{ν, fχsOpt[ν]}, {ν, Δ, 1},
  PlotStyle → {Thickness[0.008], Dashed, Black}],
 Graphics[{PointSize[0.03], Black, Point[{νopt, fχsOpt[νopt]}]}]]
```

Out[ ]=